# 2012

SALEKHARD

RUSSIAN FEDERATION

X INTERNATIONAL CONFERENCE ON PERMAFROST

## TICOP EXCURSION GUIDEBOOK

Salekhard, Yamal-Nenets Autonomous District, Russia
June 25-29, 2012

**TENTH
INTERNATIONAL
CONFERENCE
ON PERMAFROST**

**POLAR URALS:
GLACIERS AND
PERIGLACIAL
GEOMORPHOLOGY**

2012

Mikhail N. Ivanov

# Polar Urals Glaciers
# and Periglacial Geomorphology

**TICOP Excursion Guidebook**

M.N. Ivanov Polar Urals Glaciers and Periglacial Geomorphology. TICOP Excursion Guidebook – Tyumen, Russia: Pechatnik, 2012. – 50 p.

# CONTENTS

## INTRODUCTION

The Ural Mountains are aligned in the meridional direction and extend from the Pay-Khoy ridge in the north to the Ural River in the south for almost 200 km. The width of the Urals is approximately 50 km near the Polar circle and 150 km at the southern edge of these mountains. The Urals are divided into the Polar, Nether-Polar, North, Middle, and South Urals. The highest summit of the Urals (Narodnaya mountain with a height of 1894 m) is located in the Nether-Polar Ural. The Urals serve as a natural obstacle for humid air masses from the Atlantic Ocean, which is responsible for the high level of precipitation and humidity on the windward (western) slopes where glaciers are located. The Polar Ural (Fig. 1) is located in the extreme north-east of the European
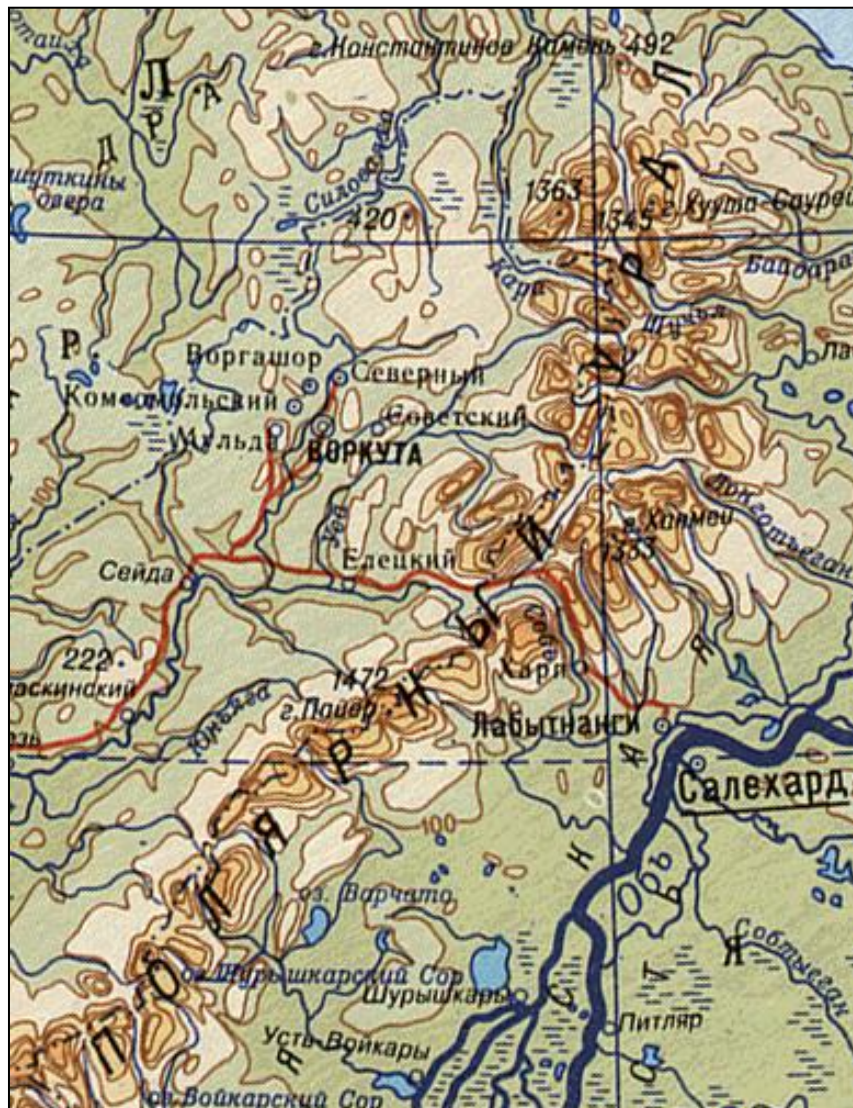


FIGURE 1. Polar Urals map.

territory of the country and extends in the north-east direction from the Kolokol'nya (Bell Tower) mountain in the south-west to the Konstantinov Kamen' (Konstantin's Stone) mountain in the north. The eastern and western boundaries of the Ural region are with the West-Siberian and East-European plains, respectively. The southern boundary coincides with the boundary between the Khanty-Mansi and Yamalo-Nenets autonomous okrugs (districts). In accordance with administrative division, the territory refers to the Komi republic and Yamalo-Nenets autonomous okrug.

The Polar Ural is the only region in the Russian Subarctic with comprehensive monitoring of mountain glaciation and environment as a whole. Glaciers of the Polar Ural are important for observations of the glaciation evolution in the north polar area and can be used as indicators of regional changes in the climate and snowiness. Glaciation exists owing to close relationships between the relief and climate. Glaciers are located below the snow line and rapidly respond to climate changes. The main information on Polar Ural glaciation was obtained by stationary observations of researchers from the Institute of Geography of the Russian Academy of Sciences in 1957-1981 in the upper reaches of the Bolshaya Khadata (B. Khadata) river basin (Fig. 2).
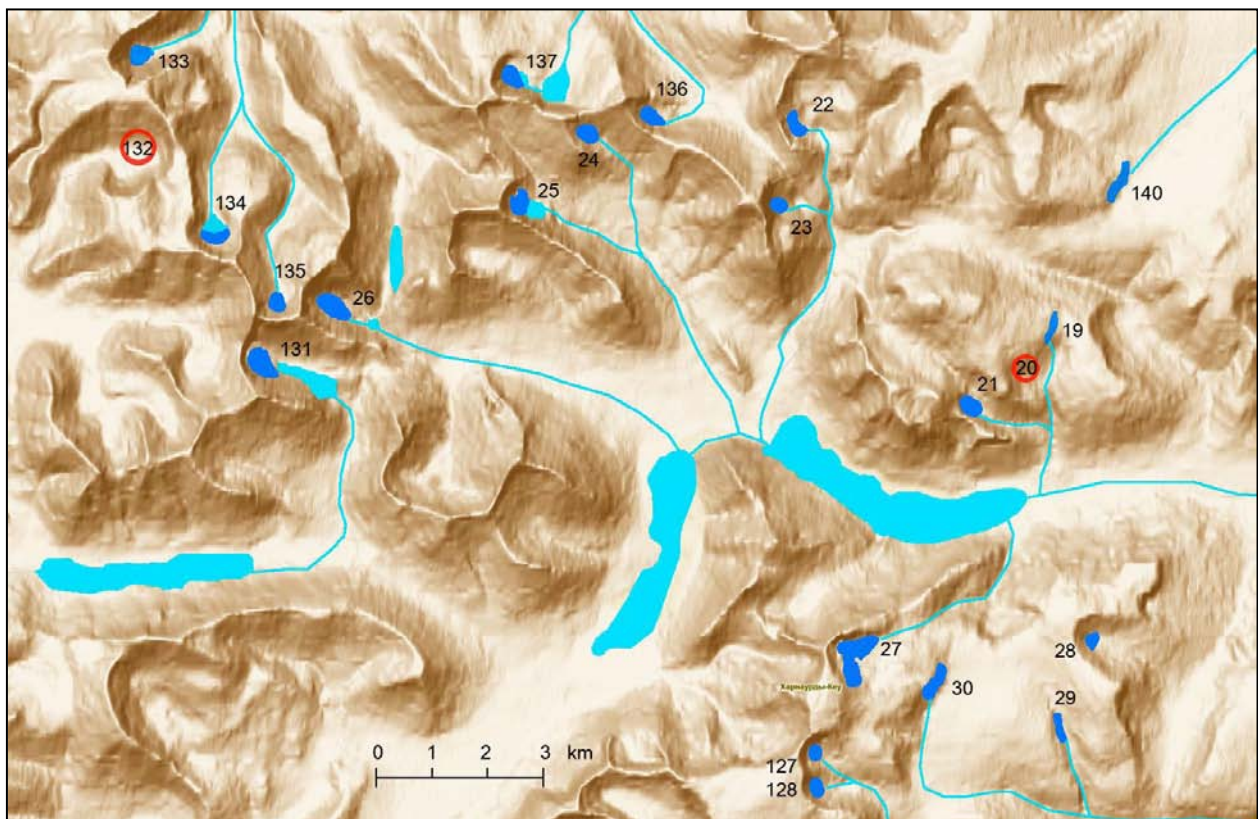


FIGURE 2. B. Khadata River basin.

## CHAPTER 1. Relief.

The Urals were formed in the period of Hercynian orogeny; during the Mesosoic period, it experienced intense denudation, which leveled off the high-mountain area to a peneplain. This process was also assisted by marine transgressions (Upper Jurassic, Upper Cretaceous, and Paleogenic), which covered the marginal areas of the Ural peneplain and, occasionally, the watershed region as well. In the Mesosoic period, the Urals experienced multiple arch uplifts, all of them being finalized by peneplain formation. In the Oligocene and Miocene periods, large arch and arch-block uplifts occurred in the Ural peneplain area, resulting in the formation of an orographically expressed mountain range. The total positive motions during the Neocene and Quaternary periods in the northern regions of the Urals are estimated at 700–1000 m. In terms of the relief and geological structure, Troitskii divided the Polar Ural into drastically different northern and southern parts [Ural Glaciation 1966].

The northern part of the Polar Ural begins from the Konstantinov Kamen' mountain (492 m) in the form of a narrow (5–7 km) ridge 500–600 m high; further to the south, it abruptly expands at the latitude of 68°20' and extends as a band 60–70 km wide toward the valley of the Sob' River where the railroad passes. The ridge width reaches 100 km in the region of the Ngane-Pe massif. The absolute heights of the ridges in the northern part of the Polar Ural do not exceed 1000–1200 m, and only some individual peaks reach more than 1300 m. The depth of dissection of the northern part of the Polar Ural is extremely large (Fig. 3). The bottoms of valleys and depressions between mountains even in the central part of the ridge often have the same absolute heights as the lowlands adjacent to the mountains. The through-pass valleys in the upper reaches of the Sob', B. Khadata, M. Usa, and M. Kara rivers are located at 150-250 m above the sea level [Ural Glaciation 1966].



*Photo by M.Ivanov*

FIGURE 3.  Alpine relief.

The transverse and longitudinal river valleys and depressions dissect the mountain surface into individual ridges and massifs; prominent ridges in this relief are the Oche-Nyrd, B. and M. Paypudynskii, Khanmeiskii, and Kharbei ridges, Engane-Pe and Borzov massifs, etc. Sometimes, high ridges are separated from each other by vast depressions up to 3–4 km wide (Paypudynskaya and Niyayuskaya depressions) or by wide river valleys with flat bottoms (upper reaches of the Shchuch'ya, Longot'eran, Baidarata, and other rivers). Many river valleys, vice versa, are narrow, have a canyon-shaped profile, and acquire the form of a gorge in the upper reaches. When reaching the main valley, the tributaries form large alluvial cones, which often are the main reason for the formation of large choked lakes in the upper reaches of rivers (B. and M. Khadata-Yugan-Lor, Usva-Ta, B. Kuz'ta, etc.). There are also tectonic lakes: B. and M. Shchuch'e [Ural Glaciation 1966]. A typical orographic feature of the northern part of the Polar Ural is the asymmetry of the main watershed, which is substantially shifted to the west. The western slope of the Polar Ural is steeper than the eastern slope. Almost over its entire length, it abruptly goes down to submountain depressions (Karskaya and Usinskaya depressions) separating submountain ridges (height 250-300 m a.s.l.) from the foothills. The eastern flank goes down gradually, sometimes in several tiers, to the wide band of submountain ridges (Fig. 4), which are weakly uplifted areas of the trans-Ural peneplain with heights of 300–350 m a.s.l.

The western part of the ridge is appreciably more dissected than the eastern part. Along with plateau-shaped and rounded summits, there are areas with a typical Alpine relief with sharp ridges, peaks, and developed kars, which often contain modern glaciers, snowfields, and deep lakes (Fig. 5). The Alpine relief is particularly expressed in the Oche-Nyrd ridge and in the region of the B. and M. Shchuch'e and B. and M. Khadata lakes. In the eastern part, there are no kars and other glacier reliefs, which makes the western and eastern parts morphologically contrasting.



*Photo by M.Ivanov*

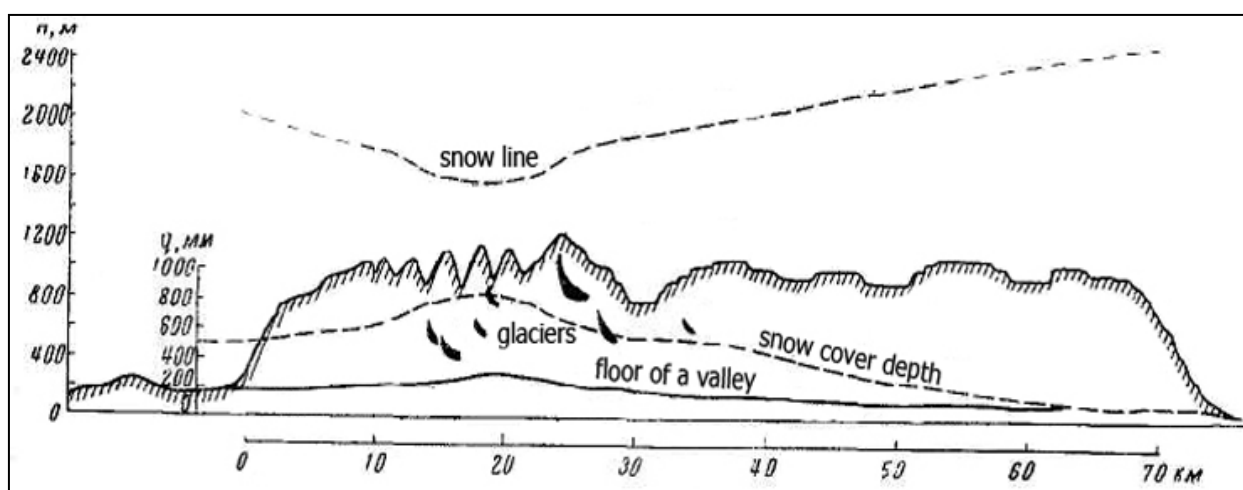FIGURE 4. Eastern flank of the Polar Urals.

FIGURE 5. Glaciogeomorphological profile [Ural Glaciation 1966].

The southern part of the Polar Ural (to the south of the Sob' river) is a substantially constricted (to 25–30 km) watershed ridge extending in the south-west direction for more than 200 km (up to the Kolokol'nya mountain). The Ray-Iz massif (Fig. 6) is located in the northern part of the ridge; the Pay-Er and Voykar-Syn'inskii massifs are located further to the south. The absolute heights of the ridge reach 1100–1200 m; the Pay-Er mountain is the highest peak of the Polar Ural (1472 m). The majority of the ridge slopes are steep and descent to submountain depressions separating submountain ridges with absolute heights up to 350–400 m from the foothills.

The southern part of the Polar Ural is a plateau with strongly dissected deep valleys, troughs, and kars. The dissection depth reaches 600–800 m. In some places, the ridge is cut by through valleys whose passes have absolute heights above 350–500 m (Khoila, Kokpel'skii, and Khaima passes). Many valleys have a typical trough character with clear signs of mountain-valley glaciation. The activity of glaciers is also evidenced by the stepwise longitudinal profile of troughs, chains of lakes supported by riegels, and powerful extreme-moraine systems.
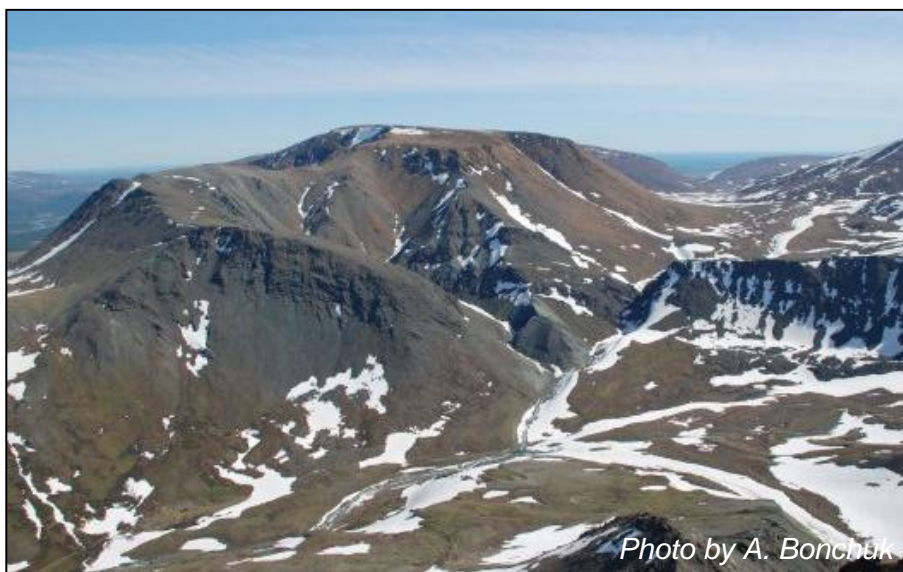


Photo by A. Bonchuk

Figure 6. Ray–Iz.

## CHAPTER 2. Climate.

The Polar Ural lies in two climatic belts: Atlantic region of the subarctic belt in the north and eastern subregion of the Atlantic-Arctic region of the moderate belt in the south. The climate of the northern part of the Polar Ural is formed under the action of arctic air accumulated above the central polar basin and air of moderate latitudes. Continental tropic air sometimes penetrates in summer when the arctic anticyclone prevails in the north-east [Alisov 1956]. The cold period coinciding with the period of accumulation on glaciers lasts from October to May (Fig. 7). The warm period (intense ablation on glaciers) lasts from June to September. At the end of September or beginning of October, there is a sudden transition from the warm to the cold period. The evolution of glaciation is affected by two major parameters: winter precipitation and its redistribution, and solar radiation responsible for changes in air temperature. The northern part of the Polar Ural is behind the Polar Circle; therefore, there is the so-called polar night in summer and the so-called polar day in winter. In summer months, the income of solar radiation reaches 150 J/cm$^2$. In winter months, the total insolation does not exceed 1.5% of the annual value [Ural Glaciation, 1966]. The most intense cyclones associated with the arctic front are observed in the mountainous northern part of the Polar Ural; further to the south, the cyclone activity is gradually attenuated. In winter, most cyclones arrive from the west and north-west along the Iceland-Kara trough.

The Urals exert a significant effect on the air flows and fronts passing over adjacent regions. First of all, it is manifested as an increase in velocity of air flows above the Urals. Owing to the high-latitude location of the region, the cold period is longer than the warm period. The mean annual temperature of air is below zero on the entire territory, and the lowest values are observed in the mountains. Representative results for the central part of the Polar Ural were obtained at the B. Khadata weather station, which was in operation in 1957-1981 at the glaciological field station of the Institute of Geography of the Academy of
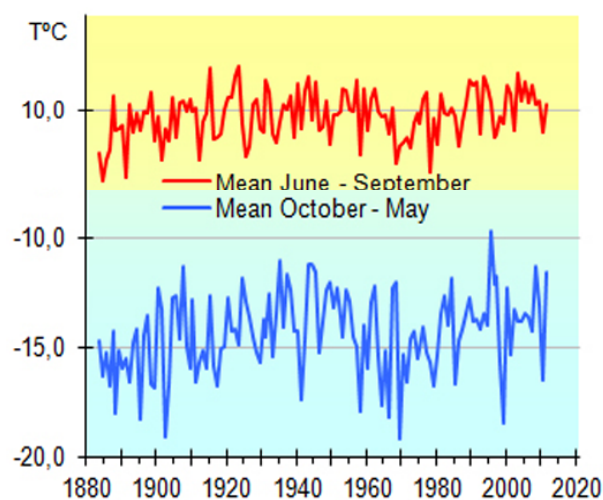


FIGURE 7. Seasonal air temperature, the Salekhard weather station.

Sciences of the USSR [Voloshina 1988]. A close correlation (r=0.9) was found between the meteorological elements measured at this station with the Vorkuta and Salekhard meteorological stations located at 80 and 100 km away from B. Khadata, respectively [Ivanov 2009]. The air temperatures measured in winter at these stations behave identically. The longest observations were performed at the Salekhard station. The mean air temperature in winter is −13°C, and the mean air temperature in the coldest month (February) varies from −18 to −25°C (Fig. 8). The absolute minimum of the air temperature (−49.6°C) was observed at the Khal'mer'yu station [Ural Glaciation 1966]. The mean air temperature in summer is +9°C. September is a transitional month when glacier ablation is equal to accumulation on the average.

Modern climatic changes lead to warming in the Urals, which stimulates melting of glaciers in the summer period. In summer 2007 and 2008, the modern microclimate on the Obruchev glacier was studied by researchers from the Poznan University [Stachnik et al. 2010, 2011]. In summer 2008, the microclimate on the IGAN glacier (named after the Institute of Geography of the Academy of Sciences of the USSR) was studied by Nosenko and his colleagues [Nosenko et al. 2009]. Analyzing the plot of the mean monthly air temperature (Fig. 8), one can trace the increase in temperature for the last four decades. In accordance with the Salekhard station results, the mean yearly temperature of air in 2001-2011 increased by 1°C (Fig. 9), the mean monthly temperature in the period from October to May increased from -14.2°C to -13.3°C, and the mean monthly temperature in the period from June to September increased from 9.6°C to 10.5°C.



FIGURE 8. Mean monthly temperature.



FIGURE 9. Temperature anomalies.
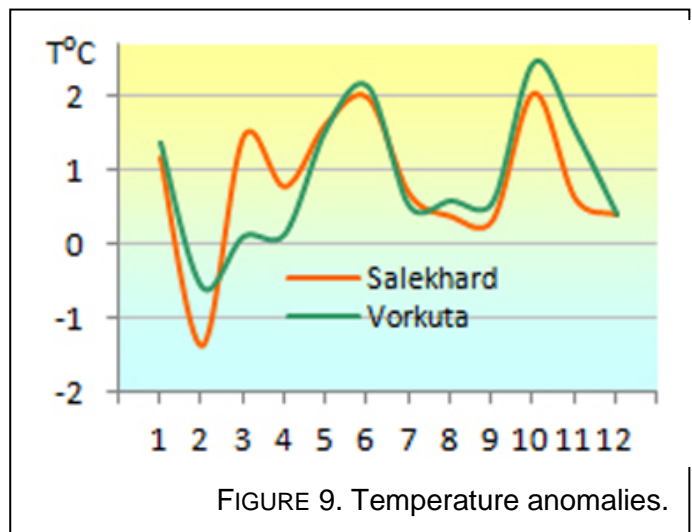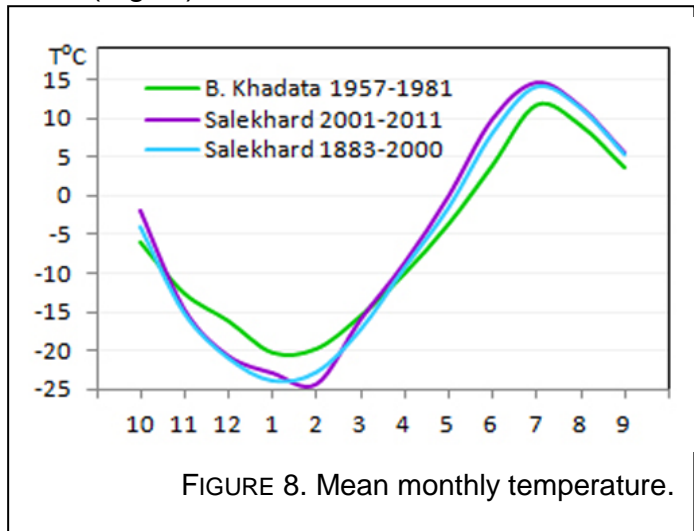
Owing to this increase in air temperature, the level of precipitation increased during the last decade, especially in the winter period. Despite its moderate height, the Ural mountain range plays an important role in precipitation redistribution. The annual amount of precipitation to the west of the Urals is approximately 1.5 times the amount of precipitation to the east of it. The amount of precipitation in the central part of the Polar Ural is three times greater than that in Salekhard, where the most reliable and regular measurements of precipitation were performed. The maximum total amount of annual precipitation based on the data measured at the meteorological station on the IGAN plateau is 740 mm on the average and can reach 1500 mm, which is confirmed by the data on the discharge of the B. Khadata river. The mean annual amount of precipitation on high plateaus (Ray-Iz station) in the eastern part of the Polar Ural is approximately 570 mm. The amount of solid precipitation at the meteorological station is underestimated approximately by a factor of 3, as compared with snow survey results [Ural Glaciation, 1966].

In accordance with the Salekhard station observations from 1891 to 2011, the period of snow accumulation lasts from October till May (Fig. 10). Winter precipitation (which approximately amounts to one half of annual precipitation) in Salekhard in 2001-2011 increased by 50 mm; the mean precipitation in winter is 240 mm (up to 700 mm on B. Khadata), as compared with the long-term standard value of 192 mm in 1891-2011.
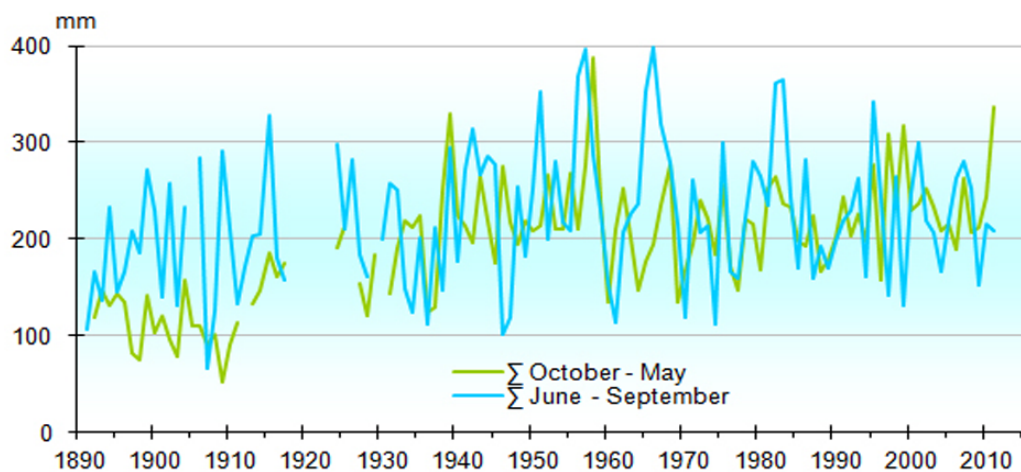


Figure 10. Long-term precipitation regime at the Salekhard weather station.

The increase in precipitation in February and March reaches 20 mm, which corresponds to 60 mm in the central part of the Polar Ural.

The increase in winter precipitation enhances the avalanche danger and exerts a favorable effect on the glacier mass balance because more than 10 m of snow are accumulated during the winter period on glaciers, which was found by stationary observations of glaciers and was confirmed by our studies in 2007 and 2009. If the current rate of climate changing is retained, solid precipitation can decrease owing to the longer warm period; as a result, precipitation in the form of rainfall is expected to prevail, and ablation is expected to become more intense.
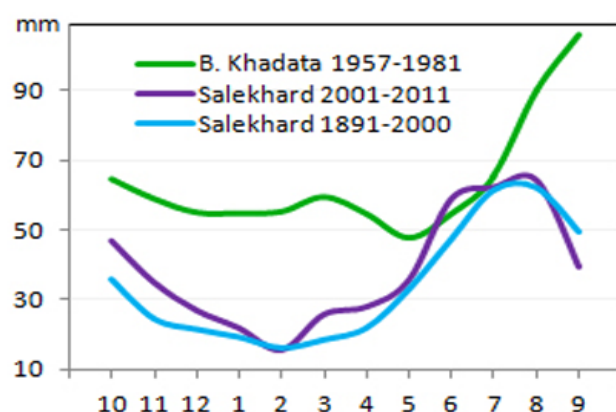
FIGURE 11. Mean monthly precipitation.

## Chapter 3. Snow cover.

A stable snow cover at the Polar Ural foothills is formed in late September – early October. In mountains, it is formed earlier, in accordance with the absolute height and latitude. The highest areas of the Polar Ural are covered with snow in late August – early September (Fig. 12). In early winter, one can see a clearly expressed snow boundary on the mountain slopes, which gradually descends to river valleys. There are frequent wet snowfalls; wet snow gets frozen and forms a dense crust almost not prone to deflation. On steep bare slopes and areas of particularly intense deflation, the snow crust is sometimes covered by a thin layer of fresh snow during the winter (in still weather), but soon the snow is entrained by the wind and is again deposited. Some areas, especially kar walls, stay without being covered by snow throughout the entire winter [Ural Glaciation 1966].



*Photo by M.Ivanov*

Figure. 12. Ray-Iz. August 2010.

Wind plays an important role in snow accumulation. At places shadowed from wind, the snow cover thickness increases both during precipitation and in subsequent periods if the wind strength is sufficient to induce low-levelsnowdrifts or blizzards accompanied by ground wind. In the second half of winter, snow accumulation generally ceases, mainly because of more frequent snowstorms. The period of reduction of the amount of snow on the plateau usually corresponds to the period of intense growth of the snow cover on the glacier [Ural Glaciation, 1966].

Intense melting at the Polar Ural foothills occurs in May or early June. In regions with a low-thickness snow cover, the major part of snow (sometimes, all snow) disappears before intense melting begins: during weak thawing periods and owing to evaporation. Melting in mountains begins later, depending on the region altitude. Intense melting, which is usually associated with arrival of warm air masses in the region, covers all altitudinal belts simultaneously. After the beginning

of melting and water infiltration, snow rapidly transforms to firn with numerous ice bands; the volume weight of snow drastically increases up to 0.55–0.65 g/cm³, and this value changes little during the melting period. The smallest volume weight equal to 0.03 g/cm³ was measured in fresh snow that fell down in still weather. The greatest volume weight equal to 0.56 g/cm³ was measured in dense medium-grain snow lying on previous year's firn at a depth of about 9 m (firn basin of the IGAN glacier). In surface horizons of the snow cover, the greatest volume weight up to 0.40–0.45 g/cm³ is observed in snow boards and loose fresh snow on dunes after blizzards. In the low horizons, the smallest volume weight is observed in depth hoarfrost. If the snow cover is not too thick (less than 0.5 m) the volume weight of depth hoarfrost ranges from 0.12 to 0.15 g/cm³ [Ural Glaciation 1966].

The amount of snow accumulated on the glacier by the maximum snow accumulation period is one of the most important components of the material balance of the glacier and is responsible to a large extent for the motion velocity of the latter, its temperature distribution, and its microstructure (Ural Glaciation, 1966). Specific features of snow accumulation on glaciers (Fig. 13) and its redistribution by blizzards form a particular glacier structure and affect glacier expansion/contraction and its front position.

Ural glaciers continue to exist despite the global climatic trend, which is favored by sufficient snow accumulation and shadowed location. During the last decade, the air temperature significantly increased, which enhanced ablation and led to glacier contraction, which cannot be compensated by precipitation enhancement during the same period.
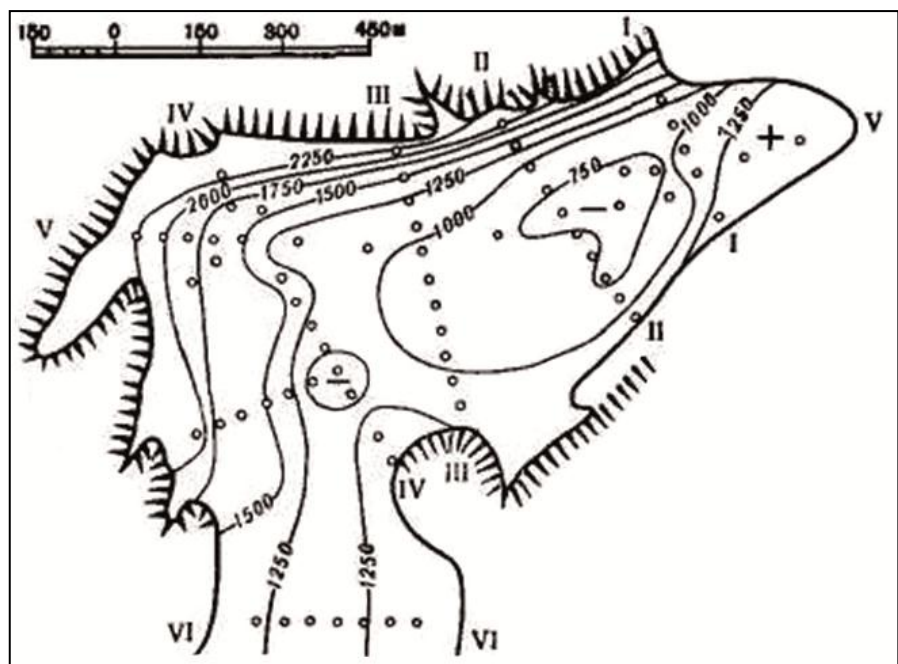


FIGURE 13. Water content in the snowpack on the IGAN glacier (mm) in spring 1960 [Ural Glaciation 1966].

## Chapter 4. Permafrost.

Specific relief and climate features ensure conditions for existence of permafrost in the Polar Ural. The permafrost thickness on bedrock flanks of mountains has not been adequately studied. The permafrost thickness reaches tens and hundreds meters (up to 400-500 m in the north), and the greatest thickness is observed in rock massifs [Popov 1967]. Loose sediments are not too thick; they are represented by bouldery loamy moraine, gravitational coarse-grained deposits, and diluvial-solifluction loamy sand materials on the mountain slopes and by alluvial coarse-grained and silt-peaty deposits in the valleys. Owing to the elevated concentration of snow in the western and central parts of the mountain range, the depth of seasonal freezing and the permafrost thickness (within 100-150 m) are smaller than those on the eastern slope, which has smaller amounts of snow and lower temperatures (250-300 m). The permafrost temperature strongly varies depending on hydrogeological conditions.

Geological exogenic processes, mainly cryogenic processes, make significant contributions to transformations of polar landscapes, forming various relief shapes; under severe geocryological conditions of the Polar Ural mountains, these processes induce various cryogenic phenomena. Temperature-gradient-induced altitudinal zoning is clearly manifested in changes of vegetation on the slopes; moreover, cryogenic processes and phenomena on slopes with different exposures are somewhat different, thus, forming different segments. Under circumpolar conditions, the northern slopes experience the lack of sunlight and have poorer vegetation, which leads to intensification of cryogenic processes. The cryogenic processes on the mountain slopes include stone runs, solifluction, landslides, and soil creep. Solifluction terraces and swells are particularly well developed on the slopes of the southern exposure owing to soils having higher temperatures (Fig. 14d). Stone runs reaching tens of meters in width, creep, and cryogenic desertion are more developed on the slopes of the northern exposure. The shapes of the polygonal and heaving relief in mountain valleys are weakly expressed and are mainly located at the foothills. Some mounds up to 2 m high were found and described in the region of the B. Khadatinskoe lake and in the upper reaches of the B. Lagorta river [Surova et al., 1975], on the eastern branch of the Rai-Iz massif [Kashkarova et al. 1999], and in the Chernaya Gorka (Black Hill) area located 2 km to the north from the Polyarnyi village [Jankovska et al. 2006]. The surfaces near the mountain tops have cryostructural relief shapes formed by frost sorting of materials: stone rings and polygons (Fig. 14b), stone bands up to 20 m long,

and spots (Fig. 14c). Thaw water from snowfields and slope glaciers play an important role in the formation of these stone bands (Fig. 14a). Cryogenic congelifraction plays a key role in the formation of nival relief shapes: kars, cirques, niches, benches, and highland terraces. The size of these shapes testifies to the long time of their formation (more that hundreds of thousands of years). Regions of ancient moraine sediments involve thermokarst relief shapes: kettles, depressions, downwarping areas, lakes, and hollows. Cryoerosion relief shapes (ravines and dales) are not well developed.



Figure 14. a – stone bands, b – stone rings and polygons, c – stone bands, d – solifluction.

Owing to favorable frost conditions, the Polar Ural has a wide range of cryogenic relief shapes ranging from large shapes (planation surfaces, cirques, kars, trough valleys, karlings, and highland terraces) and middle-scale shapes (stone runs, stone seas, moraine lines, and frost mounds) to small-scale shapes (solifluction, landslides, spots, etc.). A stable cryonival complex of relief shapes has been formed by glacier activities, cryogenic weathering and sorting, solifluction, erosion due to thaw waters, etc. Despite the recent climatic changes the intensification of cryogenic processes in the mountains is not clearly observed; it is mainly fixed as increasing of the seasonal thawing.

## CHAPTER 5. Glaciation.

In 1929, geologist Aleshkov discovered the first glaciers of the Nether-Polar Ural on the Sablya ridge. In 1930, geologist Padalka discovered the first glacier in the southern part of the Polar Ural, on the eastern slope of the Pay-Er massif. In 1945-1953, more glaciers were gradually discovered by various researchers. Dolgushin found dozens of glaciers in the region of Khadatinskoe and Shchuch'e lakes. Many glaciers were discovered by Troitskii in 1957-1960 [Ural Glaciation, 1966]. In 1956, within the framework of the International Geophysical Year (IGY, 1957-1959), the Polar Ural Expedition of the Institute of Geography of the Academy of Sciences of the USSR was organized and started its activities since 1957 at the base complex built on the bank of the B. Khadata lake (Fig. 15, 16).

During the IGY, International Hydrological Decade (IHD, 1965-1974), and International Hydrological Program (IHP), processes of accumulation, ablation, material balance, discharge of melted glacier waters, thermal balance, temperature regime of ice and snow, snow diagenesis, and ice motions were studied on chosen reference glaciers. The structure of glaciers, their geomorphological activity, and traces of ancient glaciations were examined; phototheodolithe survey of some glaciers was performed. The distributions of the snow cover



FIGURE 15. Khadata station of the Institute of Geography of the Academy of Sciences of the USSR (1960s).



FIGURE 16. Expedition on the IGAN glacier (1970s).

along the entire Ural range, in valleys and plateaus, were stu-died with the use of snow survey to identify the climatic conditions of the existence of Ural glaciers [Ural Glaciation 1966].

Modern glaciation of the Urals is represented exclusively by small shapes; morphologically, it is possible to identify kar and slope glaciers, as well as snowfields. Glaciers are arranged in groups, forming glaciation sites located at the most dissected and high regions of the range (Fig. 17). The majority of glaciers are concentrated in the northern part of the Polar Ural between N68°10' and N67°30'. The second glaciation region is located in the southern part of the Polar Ural (N67°10' - N66°30').

As the main watershed in the Polar Ural is shifted to the west, the most important feature in the arrangement of glaciers is their confinedness to the western part of the mountain range [Ural Glaciation 1966]. A typical feature of the Ural glaciers is their predominant eastern orientation. The majority of glaciers (85%) are located on slopes and in kars exposed to the east, north-east, and south-east, and only 15% of glaciers are oriented to the north and south. There are no glaciers aligned in the west direction. This specific feature of glacier orientations in the cardinal directions is caused by domination of winds of the western quarter of the horizon, leading to snow redistribution and its concentration on the leeward slopes with eastern exposure [Glacier Catalog 1966].

Based on aerial photographs and ground-based studies, 143 glaciers were found in the Urals by March 1, 1964; 91 of them were located in the Polar Ural [Glacier Catalog, 1966]. At the web site of the National Snow and Ice Data Center (nsidc.org), there is information only about 84 glaciers out of 143 as of 2011; apparently, some information was lost during the data transfer from the Institute of Geography of the Russian Academy of Sciences (IG RAS).  Not all glaciers were included into the Catalog, and no new glaciers were found after 1964. Khodakov noted [Khodakov 1978] that there are 150 glaciers in the Urals and also many undocumented glaciers and permanent snow patches. In 2009, the author revealed five previously unaccounted glaciers and found that more than 20 previously known glaciers disappeared.

Contraction and vanishing of glaciers are observed under conditions of enhanced ablation (Fig. 18). The analysis of satellite images and field studies showed that 75 glaciers can be identified in the Polar Ural as of 2011: among them, there are 40 kar glaciers and 35 slope glaciers; the area of each glacier is smaller than 1 km². The glaciation area decreased since 1964 till 2011 by 5 km$^2$ (25%) and now reaches approximately 15 km$^{2.}$.

**The IGAN glacier** (called after the Institute of Geography of the Academy of Sciences of the USSR (IG AS USSR)) is the largest one in the Urals. It was discovered

square of glaciers in 1966
- 0.1 sq. km and more,
○ smaller 0,1 sq. km.

● glaciers, founded in 2009

31 ⚡ glaciers melt by 2009

• • • • mountaine ridge

——— main watershed
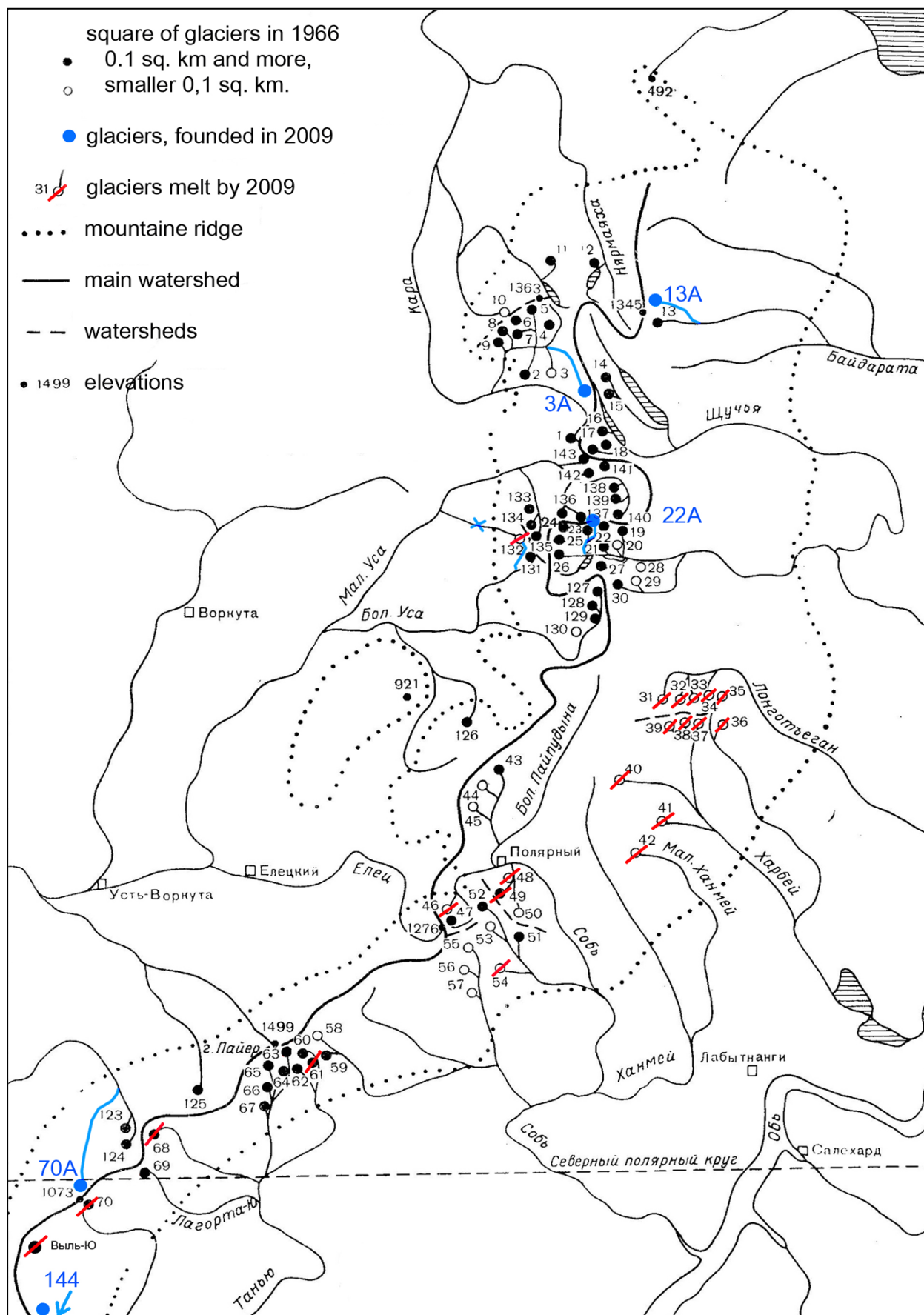
– – watersheds

•1499 elevations

Figure 17. Scheme of the Polar Urals Glaciers [Glacier Catalog 1966, changed].

in 1953 by a famous glaciologist, Doctor in geographical sciences, Leonid D. Dolgushin who celebrated his 100th anniversary in 2011. During the IGY (1957-1959), this glacier was the main site for stationary glaciological studies. At that period, the IGAN glacier had a length of 1.8 km and an area of 1.25 km². After the IGY came to an end, observations on this glacier were continued until 1981 within the framework of the IHD and then within the framework of the IHP and the program for studying glacier contraction/ expansion. The glacier description given here



Figure 18. Disappearing of the glaciers in the Minisey Mount surroundings (Kharbey-Khoy ridge). SPOT5 2009.

is based on the materials of Dr. Troitskii, the scientific supervisor of the Polar-Ural Expedition of the IG AS USSR in 1957-1977, who composed the Ural Glacier Catalog [1966], with some refinements and amendments.
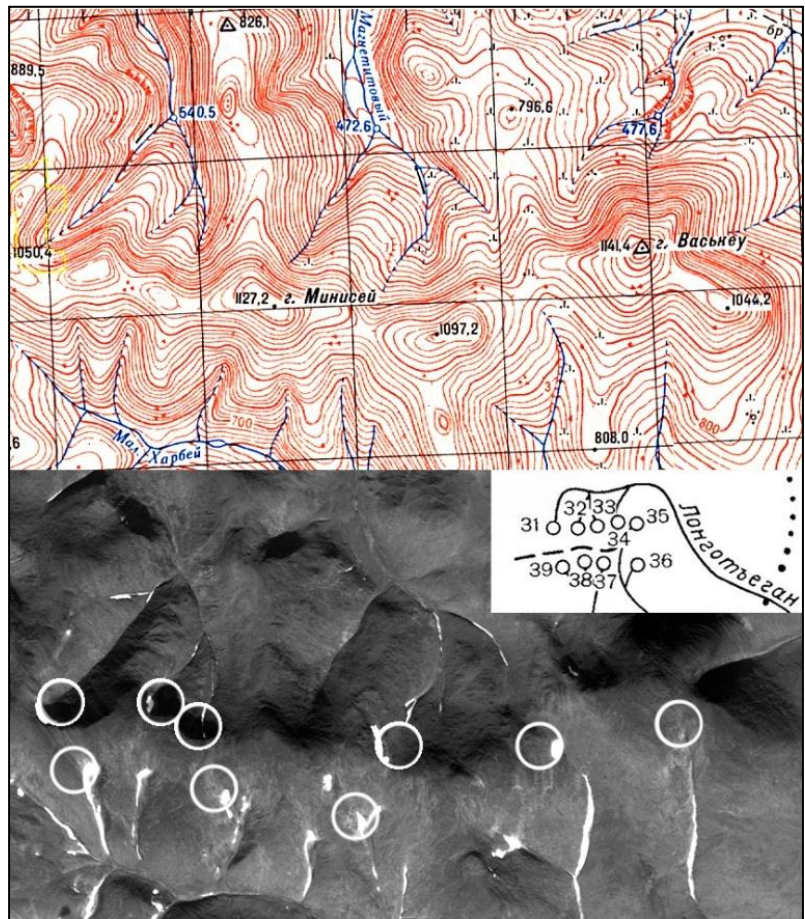


Photo by M.Ivanov

Figure 19. IGAN glacier on the slope of Khar-Naurdy-Keu, B. Khadata lake.

The glacier is located on the eastern slope of the Khar-Naurdy-Keu mountain (absolute height 1246 m), which has a flat top (Fig. 19). Its steep and strongly dissected northern and western slopes go down to the valleys of the B. and M. Khadata rivers. The relative altitudes here exceed 1000 m. From the top of the Khar-Naurdy-Keu mountain, one can see a great view of the western part of the Polar Ural with typical Alpine features of the relief: arrow-headed ridges, peaks, kars, and clefts (Fig. 20). To the east of the Khar-Naurdy-Keu mountain, there are plateau-shaped peneplain surfaces: the Medved (Bear) middle plateau with absolute altitudes of 950-1000 m; further to the east, the lower IGAN plateau with altitudes of 700-750 m, where a weather station was located during the IGY. The southern part of the IGAN glacier is located on the bare steep slope between the upper and middle plateaus; the surface of the IGAN glacier extends almost up to the plateau edge. Morphologically, this part of the glacier can be classified as a slope glacier.



*Photo by M.Ivanov*

FIGURE 20. Winter panorama to the west from the Khar-Naurdy-Keu plateau and B. Khadata river source.

Until the 1980s, the large northern part of the glacier had a well-developed tongue and was classified as a kar-valley glacier (Fig. 21); as of 2012, it is a typical kar glacier. It occupies a vast asymmetric kar deeply cut into the mountain. The steep northern and, partly, western walls (cliffs) of the kar rise almost by 200 m above the glacier surface and end with sharp ridges separating the glacier kar from the neighboring ancient kar with the Vysokoe lake (with the water level at 633 m). On the south, the glacier is bounded by the Medved plateau lying only 60-80 m above the glacier surface. The kar is open to the east-north-east. Its mouth part is somewhat constricted to a short segment of a hanging valley (about 1 km), which ends by a steep cliff. This cliff is the

basement for picturesque cascades of a glacial brook that falls into the B. Khadata river (in 3 km). Almost the entire glacier tongue is surrounded by lateral moraine banks up to 20-40 m high, which merge to form powerful terminal moraine piles approximately 400 m wide (Fig. 22).



*Photo by L. Dolgushin*

FIGURE 21. IGAN glacier, 1953.

The geological structure of the kar is clearly seen on the northern cliff (Fig. 23): it is composed from strongly dislocated metamorphic schist of the Lower Ordovician period and includes sheet deposits of basic effusive rocks. The sheet deposits are aligned in the east-south-east direction, *L* 50-60°. The metamorphic series is represented by green chlorite schist, gray and lilac cericite schist, and quarzitic sandstone. The main effusive rocks are massive gray-green amphibolized diabases. Steep sheets of the latter form sharp peaks in the north-west corner of the kar. The back wall of the kar composed from comparatively easily destroyable chlorite schist serves as a ridge, and some part of it lies 70 m lower than the plateau edge (see Fig. 21).

The slope glacier gradually transforms to the kar-valley glacier. The boundary between them (Fig. 24) can be drawn only conventionally, based on the glacier surface morphology, its structure and tectonics: stratification and directions of cracks. Water discharge from the glacier occurs in two directions: from the major part of the glacier to the B.Khadata river (Asian slope basin) and from the southern slope glacier to the B. Usa river (European slope basin). The brook originating under the southern part of the glacier sometimes runs off into the Gena-Khadata river (tributary of the B. Khadata river); it often runs off simultaneously into the B. Usa and B. Khadata rivers, thus, forming a bifurcation.
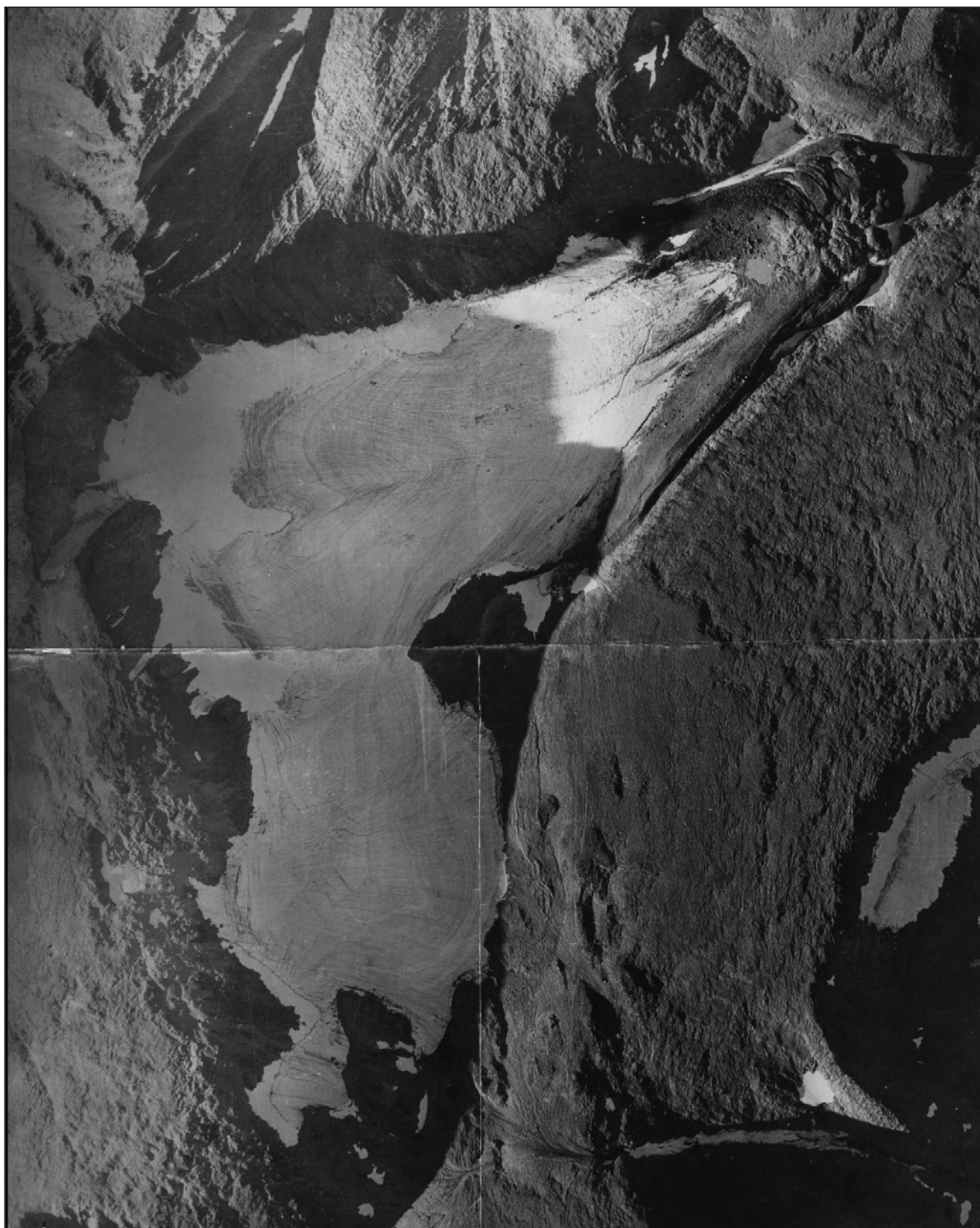
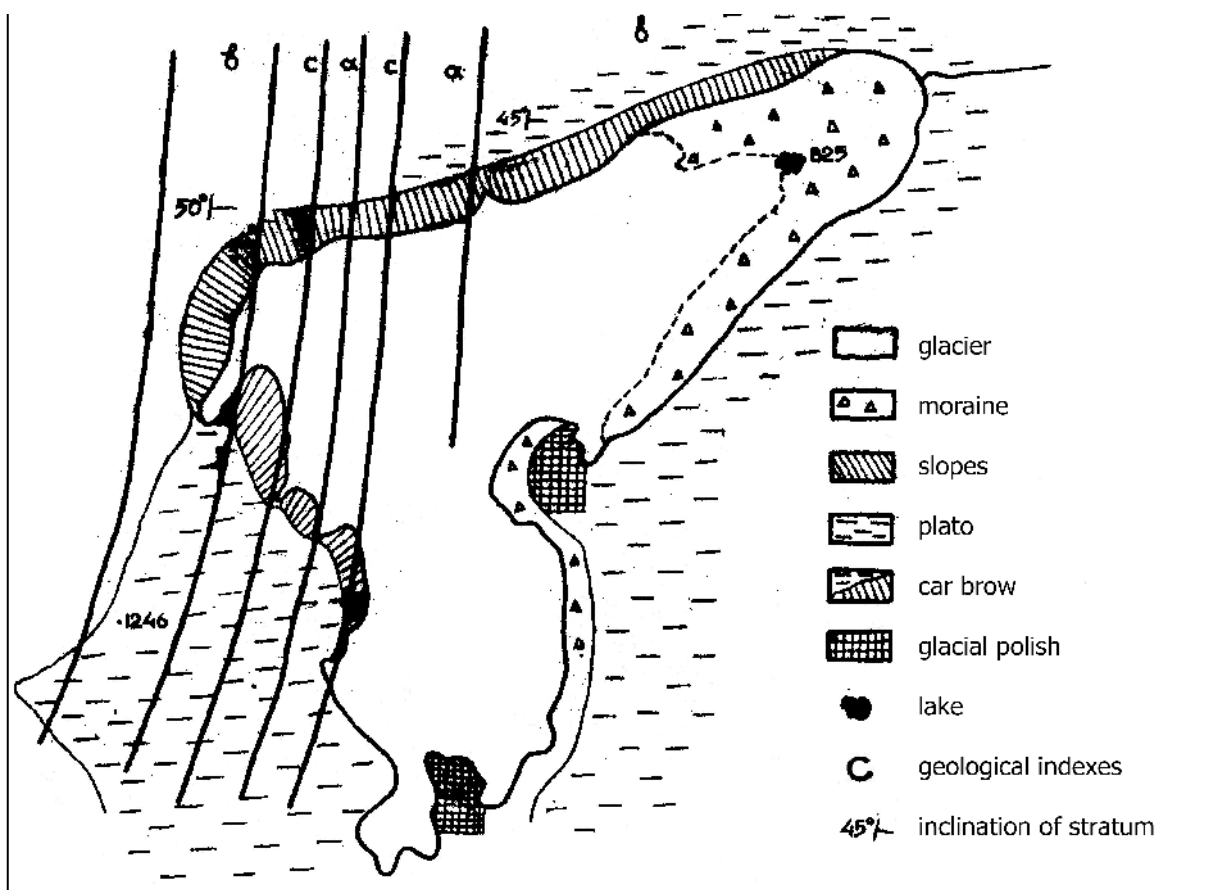Figure 22. IGAN and Medvezhiy glaciers, airphoto 1958.

FIGURE 23. Scheme of the geological structure of the IGAN glacier:
a – dislocated metamorphic schist; b – quarzitic sandstone and green chlorite schist;
c – massive gray-green amphibolized diabases. [Troitskii 1962, changed].

In the 1960-1980s, the slope glacier was up to 600 m long and approximately 900 m wide. The surfaces were inclined at 20-25°, and this angle increased to 30° in the firn basin (Fig. 26). The lower edge of this part of the glacier has the absolute altitude of 950 m, and the upper edge reaches almost the plateau brow (1200 m). The kar-valley part of the glacier together with the terminal moraine is approximately 1800 m long; its width is 600 m in the upper third and 400 m near the end of the glacier tongue, which reflects the glacier size in the period of its maximum extension more than 1000 years ago.

The absolute altitude of the foothills of the outer edge of the terminal moraine is 790 m, the absolute altitude of the end of the glacier tongue (the encroachment line of the englacial lake in 1953-1981) is 830 m, and the upper part of the firn basic reaches 1070 m. The contact line between the firn and the kar walls rises to 1150 m toward the slope part of the glacier, and the ice and firn go up to the plateau edge through couloirs and crevices in the western wall of the kar. The surface slope reach 30-35° in the upper
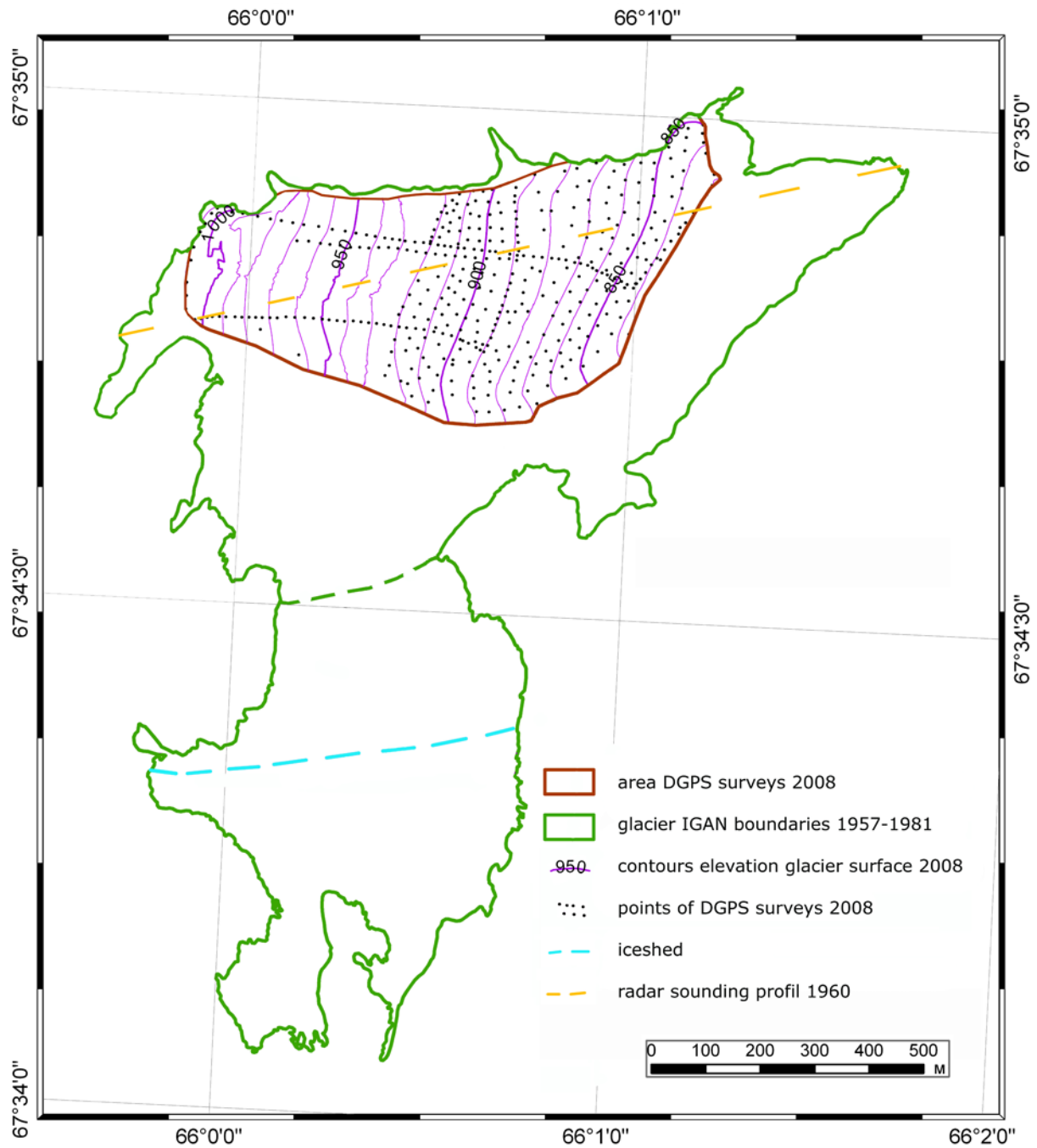
FIGURE 24. Topographic division of the IGAN glacier.

part of the firn basin, do not exceed 8-12° in the middle part of the glacier, and stay in the interval from 12 to 15° in the glacier tongue.

The firn line position and the firn basin area experience significant changes from one year to another, which is responsible for changes in snow-firn stratigraphy (Fig. 26).

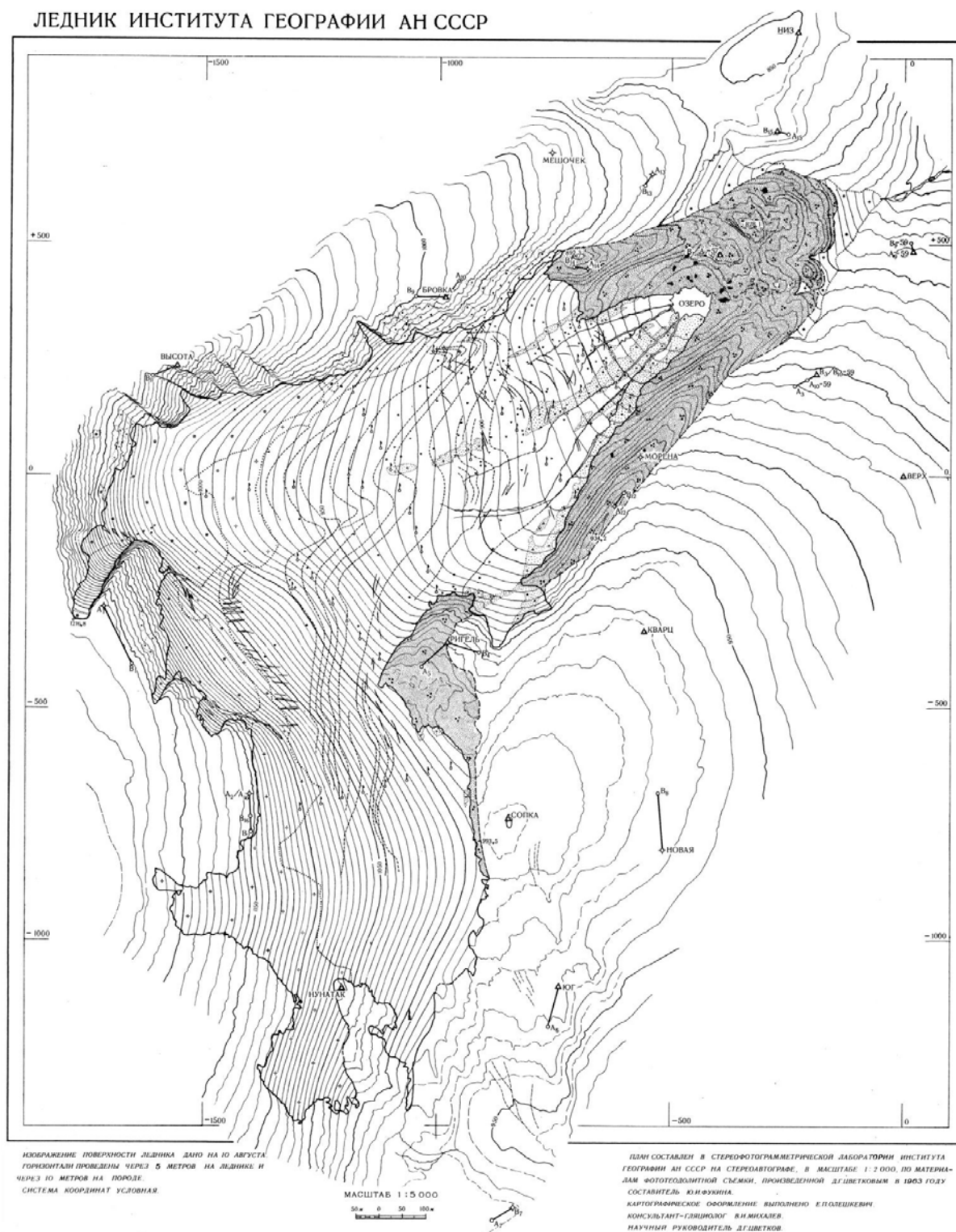ЛЕДНИК ИНСТИТУТА ГЕОГРАФИИ АН СССР



FIGURE 25. Topography scheme of the IGAN glacier, 1963 г. [Tsvetkov 1970].

Thus, the firn on the slope part of the glacier almost completely melted at the end of the ablation period in 1958, and the entire surface was covered with bare ice. In 1959, only half of the slope glacier area was free from the firn. The firn basin area in the

kar-valley part of the glacier did not experience any significant changes during these two years: it was 0.21 km² in 1958 and 0.23 km² in 1959. In I960, the firn basin area was slightly smaller. The maximum ablation during the period of instrumental observations was observed in 1976 when the firm melted almost on the entire glacier surface, and the minimum ablation was observed in 1968 when the glacier was covered with snow until the end of the ablation period.



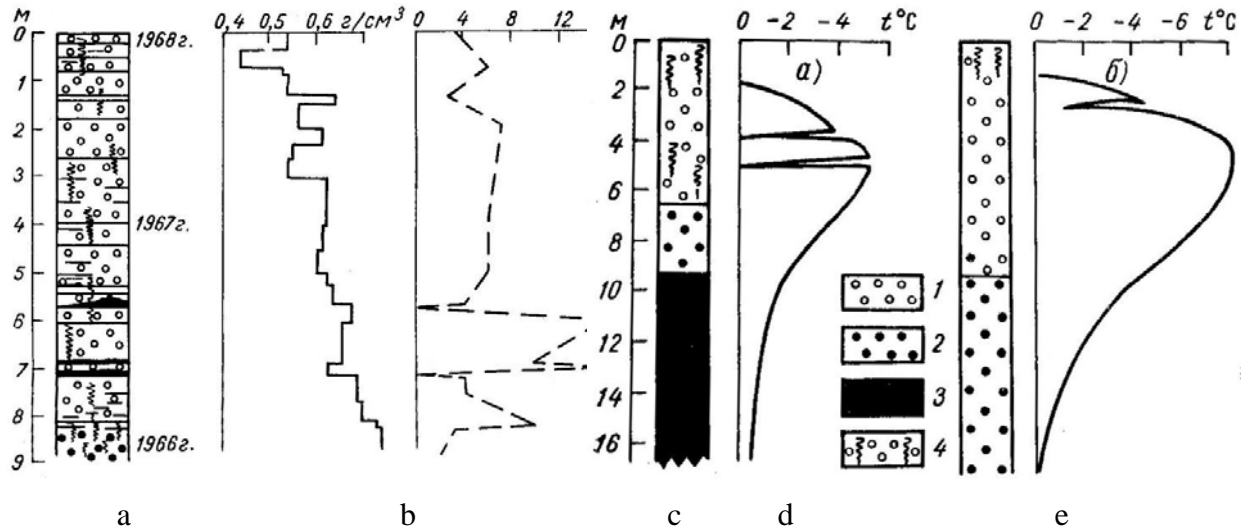a               b               c       d               e

FIGURE 26. Structure and physical parameters of firn, IGAN glacier.
1 – snow, 2 – firn, 3 – ice, 4 – moisture horizon.
a – central part of firn basin, 17.06.1968; b – upper part of firn basin 20.06.1968,
c – structural section of the upper part, 18.07.1968 г., d – density, the same location;
e – moisture content, the same location [Proceedings of the IGD].

The structural and tectonic features of the glacier are reflected in the stratification pattern, slope of ice layers, and character of crack alignment on the glacier surface (Fig. 27). There are almost straightline layers in the slope glacier with a minor subsidence in the lower third of the glacier. As a whole, the layers are aligned parallel to each other and perpendicular to the glacier surface slope. The pattern of annual zones in the kar-valley part of the glacier is more complicated. In the upper third, the layers are convex toward the back part of the kar and repeat the overall line of the firn basin. In the lower part of the glacier, the surface texture of the annual zones is deflected downward along the slope and approaches the right side. Up to 350 annual zones can be counted along the longitudinal axis of the kar-valley part of the glacier. It is rather difficult to count the annual zones at the end of the glacier because there is a large amount of clastic rocks and the layers are not always well expressed. The direction of the ice layers changes appreciably from the firn line toward the end part of the glacier. The firn layers in the firn
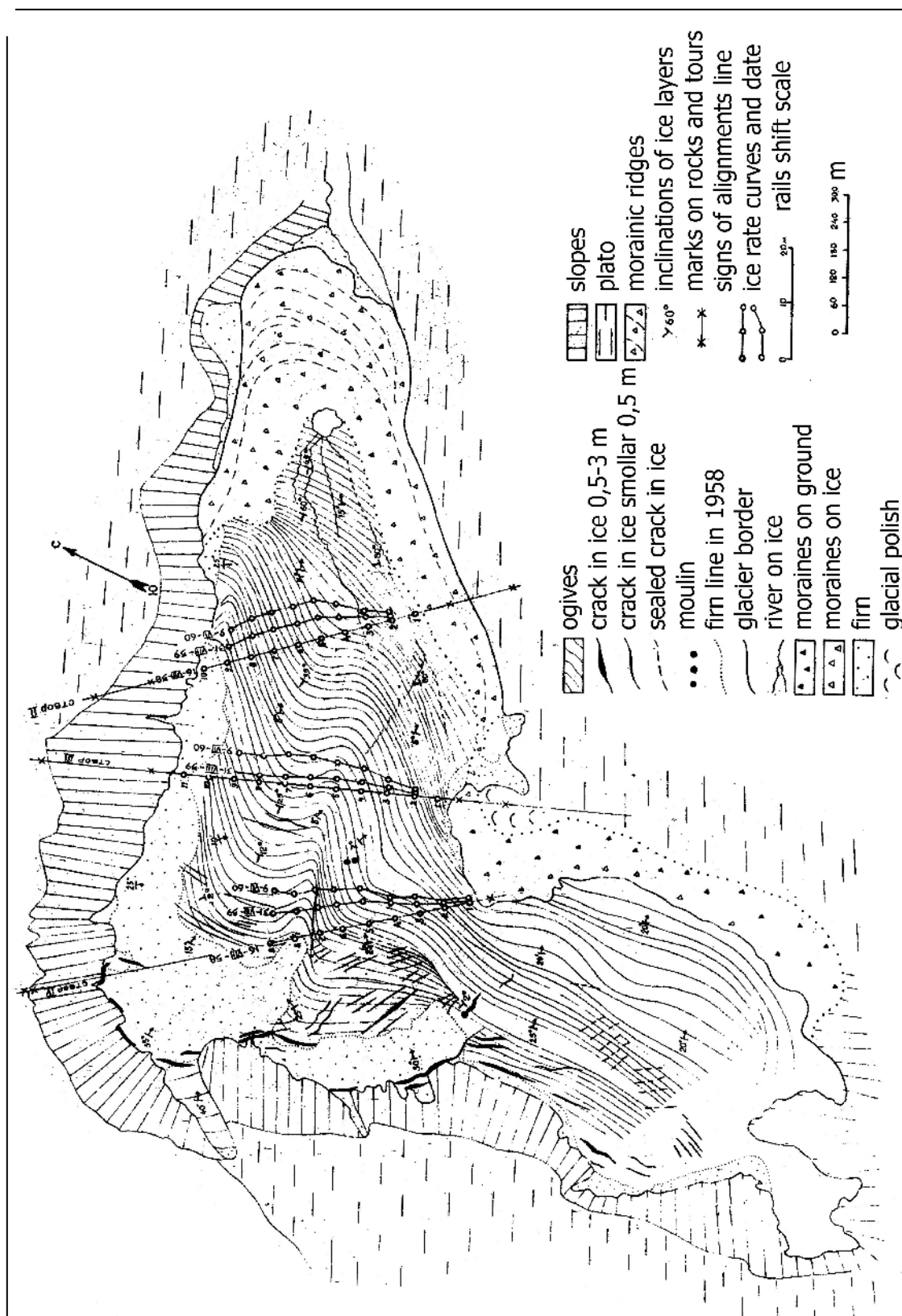
FIGURE 27. Structural-morphological scheme of the IGAN glacier [Troitskii 1962].

basin are aligned in accordance with the surface slope. The reverse direction of the ice layers (toward the back part of the glacier) at an angle of 2-4° is observed near the firn line. Then the slope of the ice layers increases along the axial line of the glacier and

reaches 65° at the end of the tongue. The layers near the right lateral moraine are aligned almost vertically (75-85°). In the upper third of the slope part of the glacier with surface slopes of 20-25°, the ice layers are aligned horizontally, and the ice layers in the lower part of the glacier have a reverse slope.

Cracks of different width mainly tend to be located near the steepest parts of the glacier. There are cracks of three types: wide cracks up to several meters with a visible depth of 10-15 m, narrow cracks from 1-2 to 5-10 cm, and sealed cracks. In addition, a continuous line of marginal cracks (bergschrund) reaching a width up to 5-7 m and a visible depth of 10-15 m at some places is located on the contact between the rocky walls of the kar and firn. These cracks are formed owing to shifting of the firn layer along the slope and become expanded owing to firn melting induced by rock heating. There are large transverse cracks in the firn basin of the kar-valley part of the glacier. In 1958, a crack up to 1.5 m wide with a visible depth up to 5-6 m was observed near the lower part of the rock outcrop in the north-west corner of the kar. The length of the open part of this crack reached 15 m, and its continuation was covered by the firn. In I960, a large crack in the upper part of the firn basin near the couloir came out from the firn. Its length exceeded 150 m, its width reached 5 m, and its visible depth was 15 m. A series of transverse cracks up to 20-25 cm and extremely narrow cracks only several centimeters wide are observed in the lower part of the firn basin and below the firn line. There are many cracks at the upper edge of the slope part of the glacier and at the place where the slope glacier transforms to the kar-valley glacier. There are both transverse and longitudinal cracks parallel to the surface slope.

At the center of the slope part of the glacier, there is a series of longitudinal cracks up to 1.0-1.5 m wide, which are sealed with transparent congelation ice clearly visible on the glacier surface. Narrow fresh and sealed transverse cracks up to 1-5 cm are encountered over the entire glacier surface. The number of such cracks in the lower part of the kar-valley glacier, however, is appreciably smaller than in the upper part. The presence of cracks on the glacier testifies that ice motion is induced not only by the viscoplastic flow, but also by block movements.

The arrangement of cracks on the glacier indicates the main directions of faults. There is a series of wells on the line of one crack; two wells are open, and others are sealed with ice. In 1953, Dolgushin observed up to ten wells here. The width of the open wells reaches 2-2.5 m, and the visible depth is approximately 20 m. They were formed

owing to capturing of riverbed flows on the glacier surface by a narrow crack. The wells are sealed by snow plugs at a depth of 15-20 m. Thus, their actual depth is unknown.

Three transverse rod lines in the upper, middle, and lower parts of the glacier were arranged in July 1958 to study the surface velocities of ice motion. Each line had 9 to 11 rods, which served simultaneously for measuring ice ablation and snow accumulation on the glacier. The ends of the rod lines were identified by special marks on the slopes and by piles of stones (cairns) on the plateau surface. The displacements of the rods with respect to the range line in 1958-59 and 1960 are shown in Fig. 27. The mark indicating the location of line III on the northern wall of the kar, which was placed in summer 1958, was not found in 1959 (a rock fragment fell down). Therefore, the measurements of line III in 1959 showed only the distance from the rods to the newly placed line rather than the magnitude of rod displacements throughout the year. As is seen from the diagram of the ice motion velocities, the greatest velocities are observed on the axial line of the kar-valley part of the glacier; they are also significant near the northern wall of the kar and rapidly decrease at the southern edge of the glacier. Observations showed that the velocity of ice motion in the upper third of the glacier is almost twice the velocity of its motion in the middle and lower parts (Fig. 28).
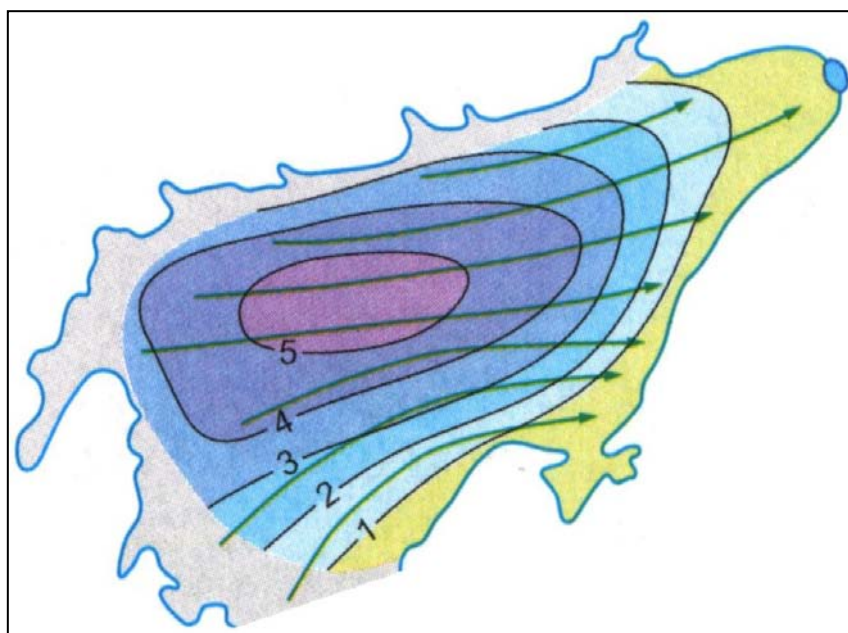


FIGURE  28. Mean velocity of the horizontal ice moving, IGAN glacier (m/yr), 1958–1981
[Atlas of the YNAD 2004].

No deep drilling for determining the ice thickness on the IGAN glacier was performed during the IGY period. Thermometric wells (Fig. 29) drilled at different places on the glacier down to a depth of 25 m did not reach the glacier bed except for two cases. At 100 m from the lower edge of the slope part of the glacier (near the second

rod of line IV), the bed was found at a depth of 12 m. In the well drilled at 150 m from the englacial lake, soil was found at a depth of 8 m. Troitskii indicated [Troitskii 1962] that it could be an internal moraine, while the real glacier thickness was greater, but ice melting on these areas in the 2000s showed that the ice thickness was not too large.
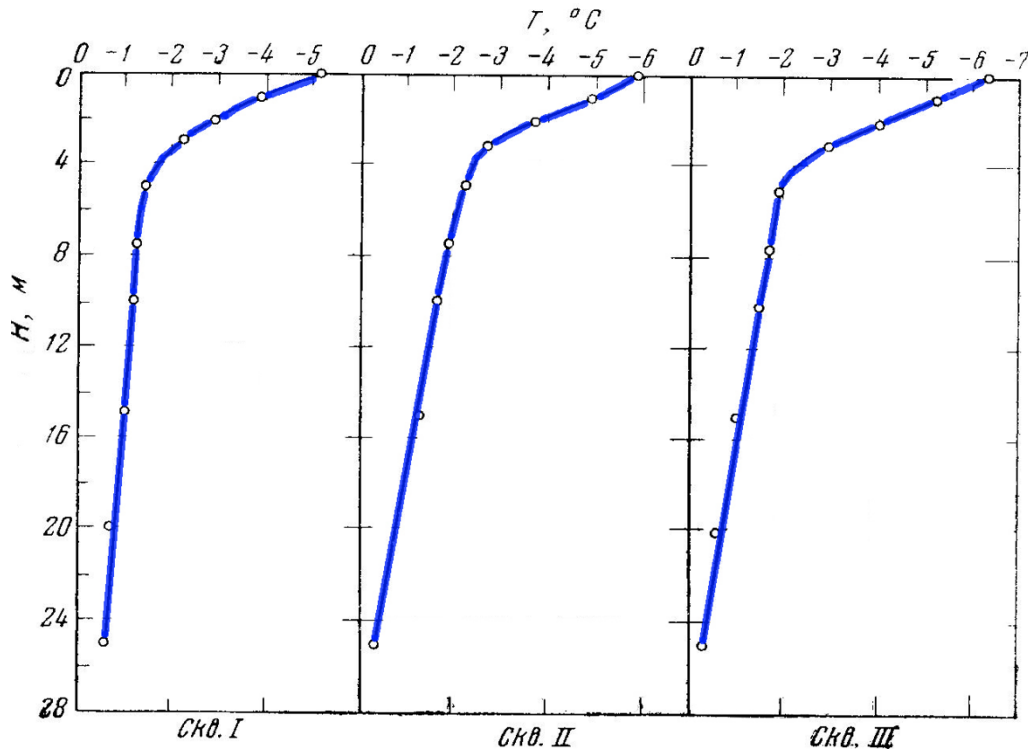


Figure 29. Temperature regime. IGAN glacier 14.01.1959 [Tsukin 1960].

Some approximate calculations of the ice thickness in the IGY period on the basis of the material balance of the glacier and ice motion velocities show that the maximum thickness of the kar-valley part of the glacier can reach 100 m near the firn line and 50 m in the region of lines III and II. Assuming that the glacier has a valley character below line III and that the glacier surface is approximately parallel to its bed, we calculated the glacier thickness by the formula derived by Max Lagally. The glacier thickness predicted by this formula was 45-47 m, which is fairly close to the value obtained by balance-based calculations. It does not seem reasonable to use the Lagally formula for the upper third of the glacier, because, apparently, there is bed incision here and the main condition for using this formula is not satisfied.

Radioprobing along one profile was performed on the IGAN glacier in 1968 (Fig. 30). The longitudinal profile of the glacier allowed researchers to conclude that the glacier stratification is determined by the difference in ice temperature; drilling revealed the interface between cold and warm ice, which is a layer with an increased moraine content [Macheret 2006]. The interface between cold and warm ice drawn in the

longitudinal section on the glacier portion contracted by 2008 is actually the boundary separating the bottom moraine-containing "ice" and merges with the homogeneous isothermal layer under point 9.
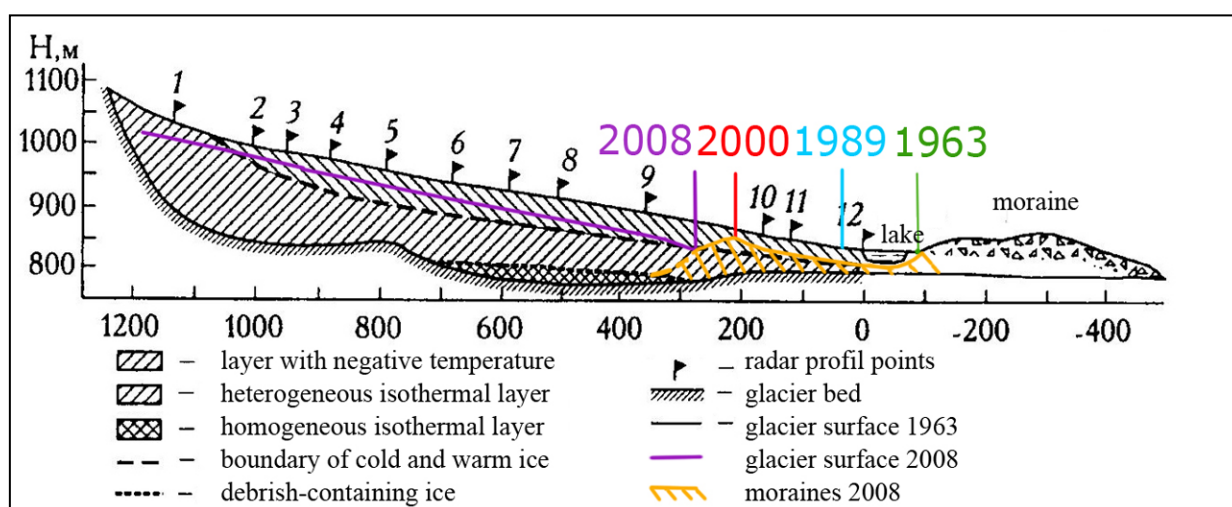


FIGURE 30. Structure of the IGAN glacier according radioprobing, 1968 (440 MHz by PB-10) [Macheret 2006, added].

Ice stratification is clearly expressed, and the layer boundaries are emphasized by increased concentrations of fine-grained soil, small fragments, and often various organic substances (leaves of dwarf birches and willows, pieces of moss and lichen, remainders of mosquitoes, etc.). These admixtures are accumulated in the period of ablation on the firn surface. The thickness of individual layers varies from 0.2-0.3 m to 3-3.5 m. Secondary stratification is observed within one annual zone, which reflects ice formation processes. The secondary layers have different colors and textures. The ice color varies from milky white to transparent blue, which is conditioned by different contents of air inclusions (Fig. 31).

In the upper part of the glacier, broken ice has a "sparkling" surface reflecting the initial granular structure of the firn. Being crushed, a piece of ice can disintegrate into individual firn grains up to 0.5 cm in size. During the ablation period, the radiation melting crust is formed on the ice surface, which is often completely similar to the porous firn. In the lower (tongue) part of the glacier, where the deep ice layers subjected to dynamometamorphism processes come out to the surface, the ice crystals are larger, ice is more transparent, and ice crushing yields a conchoidal fracture. The ice surface is not smooth; it is covered by thawing cells, stratified layers, and a fine net of small channels through which thawing water goes down across the layers (Fig. 32). At places with increased contents of fine-grained soil and small fragments, which enhance ice melting, the porosity and sponginess of the ice surface increase. Ice glasses 5-10 cm

deep are encountered. Melting is more intense on the boundary of layers, which often have a high content of cryokonite; grooves and steps emphasizing the annual lines are formed.



*Photo by M.Ocadchy*

Figure 31. Microrelief on the IGAN glacier surface, 2009.

The main surface runoff occurs through a dense net of small (10-20 cm) swash channels, which merge in the lower part of the glacier and form canyons. Some part of the runoff in the upper third of the glacier is absorbed by transverse cracks. The largest canyon extends along the foothills of the orographically right lateral moraine, reaching a depth of 4-5 m and a width up to 1-1.5 m. In the IGD period, some parts of the canyon were overlapped by ice bridges, and the brook passed in a tunnel inside the ice. Two other (shallower) canyons were located in the middle and left parts of the glacier tongue and formed moderate-size meanders; the major part of these canyons was covered by snow almost by the end of summer. In the 2000s, the lower part and the right side of the glacier tongue melted, releasing a riegel covered by the moraine and supporting a new englacial lake at a higher level.

Brooks from the glacier fall into the lower drainage lake (the absolute altitude of the lake contour is 830 m) supported by terminal moraine banks (Fig. 33). The lake is 1-1.5 m deep, and ice formed its banks and bottom in 1953-1981. The lake bottom is covered by a layer of glacier mud. The lake water has a greenish-gray color because of large amounts of glacier sediments. Directly from the lake, the flow passes between two large fragments to the sub-moraine ice tunnel; passing under the terminal moraine, the

*Photo by P. Stoykin*

FIGURE 32. The tongue of the IGAN glacier and the melting area, 2005.

flow again comes out from under its outer edge. The lake level and size experience significant changes. At the beginning of the melting period, when the sub-moraine bed is still plugged by ice and snow, the lake overflows, and its level increases by 3-4 m. The lake width reaches 150-200 m. When the snow-ice plug is broken, the lake water level decreases, and the lake diameter does not exceed 60-80 m by the end of summer. A temporal increase in the lake level occurs because of the failure of the tunnel roof; the location of the cavity receiving the flow from the lake changes from one year to another. It was located at the place of merging of the right lateral and terminal moraines in 1958 and in the middle part of the terminal moraine in 1959 and 1960.



*Photo by M.Ivanov*

FIGURE 33. Moraine of the IGAN glacier.

The right bank of the lateral moraine is approximately 900 m long with a foothill width up to 100 m; in 1960, it reached a height of 40 m above the glacier surface. It consists of non-melted ice under the morainic mantle. The outer edge of the bank is separated from the bedrock slope lying to the south from the plateau by a depression

10-15 m deep, which was formed by more intense melting of ice on the contact with bedrocks under the action of water flowing down from the slope. The ice base of the moraine bank rests against the bedrock slope. The depression bottom is occupied by a snowfield. The bank ridge is narrow; the slope angle is 35-45°. The morainic mantle in the lower part of the moraine bank is thin, and ice can be seen at some places up to a height of 7-10 m from the glacier surface. The upper part of the bank is covered by a thicker mantle of clastic rocks, apparently, up to several meters. The moraine material has different sizes: from crushed rock and fine-grained soil to huge blocks up to 4x3x2 m. Owing to ice thawing, which proceeds much slower under the morainic mantle than on the open surface of the glacier, the moraine material slips down the bank. The left side bank of the moraine is approximately 300 m long and up to 20-25 m high. It is also separated from the bedrock slope by a depression 5-10 m deep; the depression bottom is occupied by a snowfield. The moraine material covers the surface of the bank-shaped ice outcrop as a continuous mantle, preventing the ice outcrop from intense melting. Ice can be seen at some places under the rock fragments in the lower part of the bank. The glacier surface adjacent to the moraine bank is also covered by a mantle consisting of clastic rocks.

Both banks of the lateral moraines merge together, forming a powerful terminal moraine. The latter has a length up to 400 m and approximately the same width; it is a system of arched banks and ridges, as well as randomly located hills composed of coarse clastic rocks (see Figs. 22 and 33). The height of the inner edge of the terminal moraine above the lake surface reaches 10-15 m, and the height of the outer edge above the level of the brook flowing from under the moraine is 25-30 m. The banks and hills of the terminal moraine contain core ice. In summer 1958, an ice outcrop was observed at the junction of the right lateral moraine and the terminal moraine approximately at a distance of 100 m from the lake at a height of 5-7 m above the lake level. The visible ice up to 3 m thick is covered by a 1-m moraine layer. The ice is clean and transparent; it consists of large crystals. In this outcrop, the ice contains a rather small amount of fine-grained soil. The outcrop surface intensely melts, and the ice cliff shrinks with a velocity of 15-20 cm per day in some individual warm days. The moraine material lying on ice slides down along the outcrop surface to a vast ice grotto located under the outcrop and extending deep under the moraine. In summer 1959, this outcrop and grotto became occluded to a large extent.

Powerful ice layers can also be seen at other places of the inner edge of the moraine. New ice outcrops appear in different years and even in different months during one summer, while old ice outcrops become occluded. The entire surface of the terminal moraine is subjected to intense thermokarst processes. Ice lying under the morainic mantle melts and forms dips. Particularly large dips are formed owing to the failure of the sub-moraine tunnel roof washed away by the brook flowing out of the lake. This flow often migrates and expands its bed. Thus, two new 10-m dips appeared in the middle part of the terminal moraine in 1959 and 1960. Smaller dips on the moraine surface occur regularly. Thus, the moraine surface permanently changes its morphological appearance, which is an explanation for the visible freshness of the moraine. Troitskii assumed [Troitskii 1962] that the moraine banks surrounding the glacier tongue are moderate-size (presumably, 10-15 m) bands of dead ice subjected to intense destruction, though they did not yet lose relations with the main body of the glacier. The positions of the bank ridges are fairly stable in time, which allowed researchers to date the moraines of the IGAN glacier (Fig. 34) by the lichenometric method [Solomina et al. 2010].
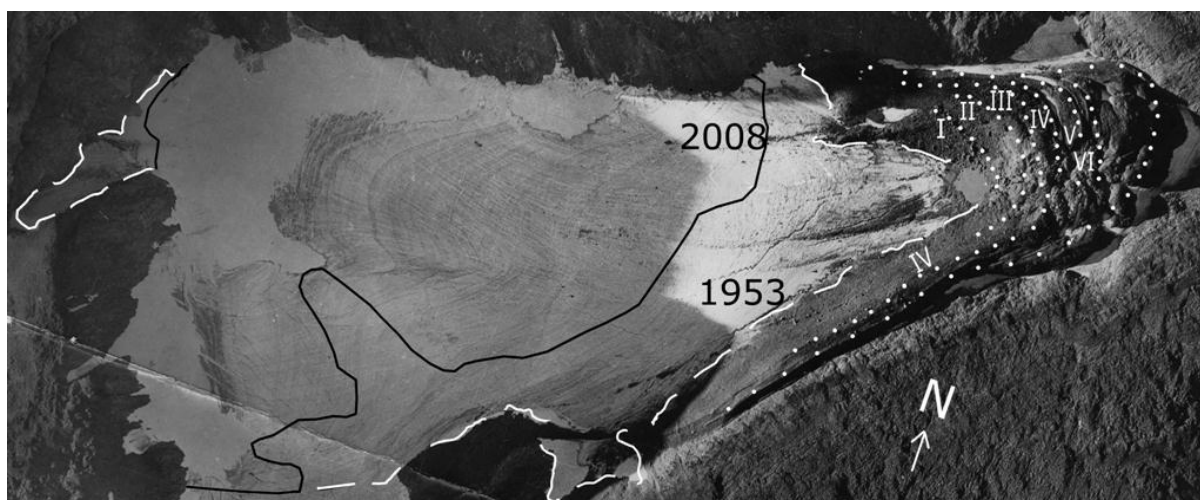


FIGURE 34. IGAN glacier, airphoto 1958. Age of moraines.
I – 1940-1950, II – 1910, III – 1890, IV – 1820, V – 1700-1600 yr., VI – 1200 yr.
[Solomina et al. 2010 changed].

The fragments of the material composing the moraine have different sizes: from clay and crushed stones to coarse fragments with individual pieces up to 5x4x3 m in size. The material is not sorted at all. The fragments mainly have angular uneven edges without any signs of roundedness. Many of them, especially schist fragments, have striations. Some fragments lying on the surface of the moraine banks have a rounded shape and look rather similar to rounded boulders. Such boulders, however, are formed

in the case considered by weathering, which made the boulder edges rounded and smooth. The fragments are composed of the same rocks as those observed in bedrock outcrops of the kar walls. Studying the bedrock outcrops and moraine composition, one can trace the main ways of transportation of the clastic material by the glacier. Thus, for instance, large fragments of dark green diabases with spotted inclusions of bright green amphibolites, which lie on the surface of the extreme and right lateral moraines, are found only on the back wall of the kar; therefore, they were brought by the glacier from that place.

The clastic material composing the moraine and lying on the glacier surface is subjected to intense frost and chemical weathering. Sericite and chlorite schist is destroyed particularly rapidly. One can observe all transitions from monolithic fragments to strongly desquamated or destroyed to such an extent that clay mass is formed if the piece is squeezed between the fingers. Depressions on the surface of large blocks often contain products of weathering of this rock: crushed stones and fine-grained soil. The process of schist weathering on the moraine surface proceeds until the stage of alumina formation. This fact explains the large fraction of the clay material in lower horizons of the moraine and the muddy water in the lake and in the brook flowing out from the lake. There are layers of glacier mud on the lake bottom and on its banks. The ice brook washes out the moraine and transports large amounts of suspended sediments.

There is a band of terminal moraine sediments along the lower edge of the slope part of the glacier; the width of this band reaches 150 m (Fig. 35). The brook passing over the depression parallel to the glacier edge washes out the moraine and opens the ice layers on which the moraine rests. The sub-moraine ice layer is no more than 1-2 m thick, and it is rapidly pinched out. The major part of the moraine material lies directly on soil, forming hills and ranges of moderate height. At the junction of the southern slope part of the glacier and the northern kar-valley part, the morainic mantle covers the bedrock outcrop. The bedrock fragments are well rounded; comparatively recently, the outcrop was covered by ice. The depression separating the outcrop from the plateau was also recently covered by ice; thus, this outcrop was a nunatak for some time.

In the lower steep part of the glacier tongue, there are two bands of middle moraines more than 300 m long. Their height is only 1-3 m. The morainic mantle is rather thin, and ice can be seen everywhere between rock fragments. The majority of the fragments are concentrated in the lower part of the glacier tongue. In the middle part of the glacier, piles of clastic rocks usually reach sizes of 5x3x1.5 m or 3x3x1 m. In the

upper third of the glacier and in the firn basin, there are only individual fragments, which rolled down from the kar walls. The main mass of the clastic material from the kar walls enters the edge cracks and is brought away by the glacier to the tongue end in the form of the bottom moraine. Some part of the material that arrived on the firn basin surface becomes submerged into the firn layer and, after passing some distance in the glacier body, melts out from the ice in the middle or lower part of the glacier, forming surface middle moraines or detritus. Only a minor fraction of fragments arrives on the glacier directly from the kar walls by sliding over the firn surface.
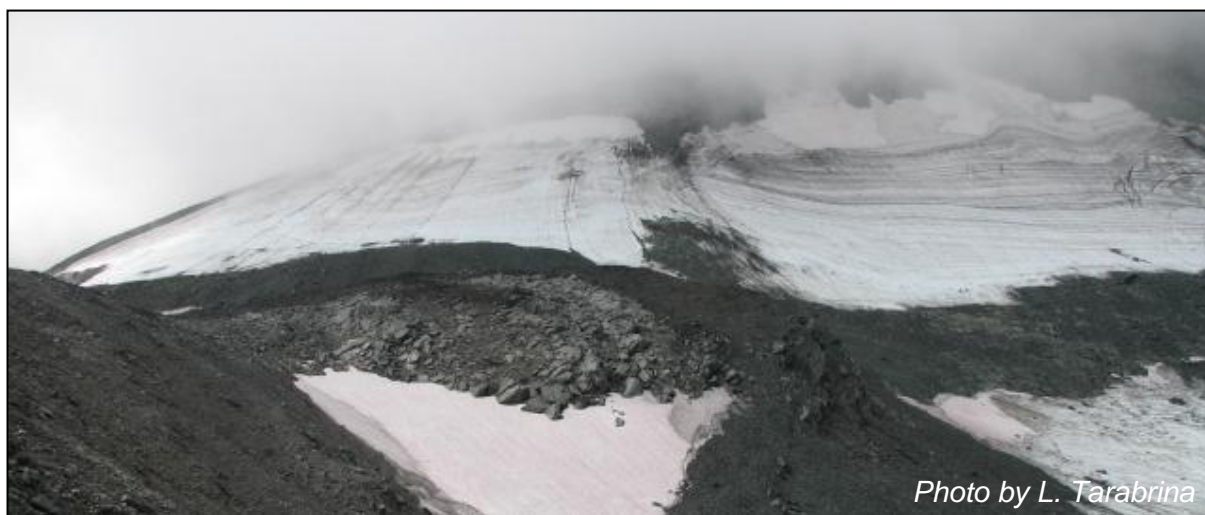


*Photo by L. Tarabrina*

FIGURE 35. Moraine and rocks in the contact of the slope and kar-valley parts of the IGAN glacier, 2007.

The clastic material on the glacier surface moves not only because of ice motion in the glacier; it can also move independently. Large fragments prevent the ice surface from the action of direct solar radiation, the ice under such fragments melts more slowly, and an ice mushroom or table is formed. The height of the ice leg of the table is usually 40-50 cm, sometimes reaching 60-70 cm, which depends on the fragment size and shape. After that the fragment slips down from the ice pedestal, usually in a direction somewhere between the surface slope direction and the direction to the south where the maximum intensity of direct solar radiation is reached.

Staying on the glacier, one can directly observe kar wall destruction mainly induced by frost weathering. Frequent transitions of temperature through zero in both directions, which ensure numerous alternating freezing and melting of water in rock cracks and pores, lead to intense destruction of rocks. These processes are manifested to the largest extent in the anticyclone weather when the rocks cooled down to a low temperature during a still night without clouds are rapidly heated by the Sun in the morning. In such periods, one can permanently hear noise generated by falling rock

fragments. Screes and moderate-size mud-stone avalanches reaching the firn surface often occur. A large number of fragments separated from the rocks by frost weathering hardly stay on the kar walls. Bands of screes go down the clefts in the kar walls; they can be set into motion by a small stone rolling down these screes. Enhanced weathering occurs on the contact line between the firn and the rocks in marginal cracks. The products of frost weathering are entrained by the glacier to the kar mouth; thus, the back part of the glacier moves deeper into the back wall of the kar and makes it step back. Owing to this backward motion, the back wall of the kar has the form of a ridge, which continues to destroy and to lose its height. Some part of the ridge lies 70 m lower than the plateau level. On one segment of the ridge lying at the altitude of the Khar-Naurdy-Keu plateau still has an area up to 30 m wide (remainder of a plateau).

Since the beginning of observations in 1953, all researchers noted degradation of the IGAN glacier, which started after the maximum of the Little Ice Age and short-time periods of glacier expansion in the 19th century. The long-time period of glacier degradation is evidenced by high lateral (up to 40 m in 1960) and terminal moraines with ice cores, which indicate the previous level of the glacier surface.

In 1957–1981, the mass balance was measured on the IGAN and Obruchev glaciers (Fig. 36). During the 24 seasons of observations, the mean annual mass balance of the IGAN glacier was negative: -40.0 $g/cm^2$. The level of accumulation-ablation at the equilibrium line (800 m on the average) is approximately 200 $g/cm^3$·year. The vertical gradient of external mass transfer is 22 $g/cm^2$·year per one meter of altitude. The ice formation zones are the warm firn, firn-ice, and ice zones [Atlas of Snow and Ice Resources 1997].

The contrast of meteorological conditions in winter and summer caused by the geographical position of the region is responsible for high oscillations of the mass balance components of the Polar Ural glaciers (Fig. 37) and its total value from one year to another.

The close relationship of accumulation (r=0.83) and ablation (r=0.86) with the mean seasonal temperatures of air measured on the nearby meteorological stations made it possible to reconstruct the glacier mass balance for the last 200 years by extrapolating the series of observations of the IGAN glacier evolution (Fig. 38).
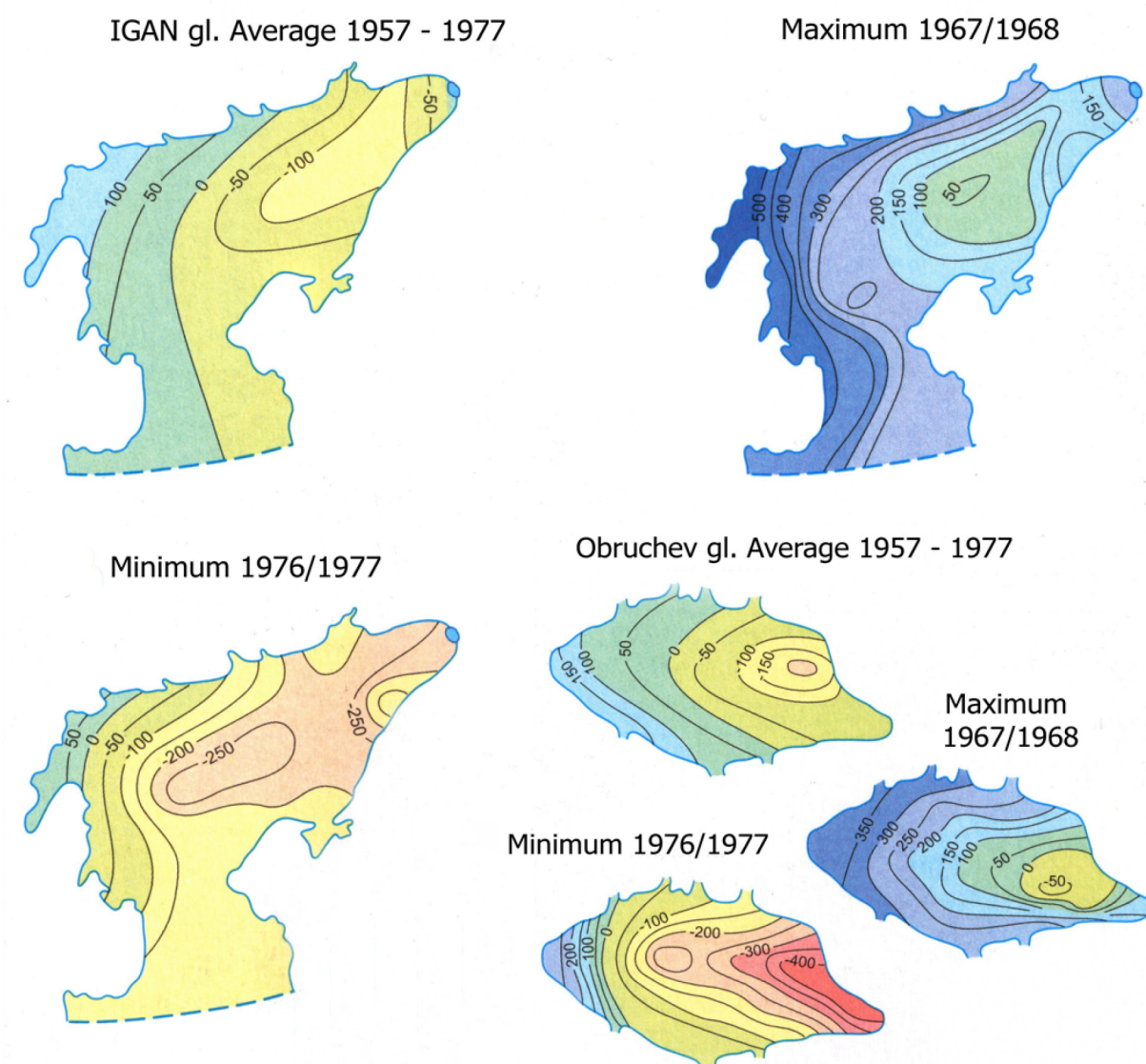
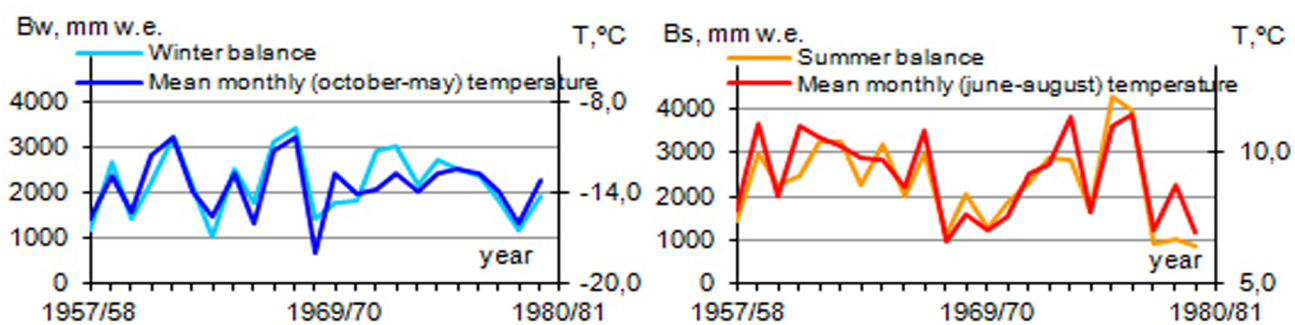FIGURE 36. Mass balance of the IGAN and Obruchev glaciers [Atlas of the YNAD 2004].



FIGURE 37. Measured accumulation (Bw), ablation (Bs) of the IGAN Glacier.
Air temperature X–V and VI–VIII, Vorkuta weather station.

A comparison of aerial photographs and topographic plans of the glacier in different years reveals significant changes in the glacier size and shape (Fig. 39). The lower edge of the slope part of the glacier moved 40-80 m away on different areas in

1953-1958. A large ice portion at the upper edge melted, and the area of the extreme southern end of the glacier appreciably decreased. By 1960, the edge of the slope part of the glacier moved away by 100-150 m, and the ice thickness decreased correspondingly. In the 1970s, the glacier remained in a stationary state, followed by the next period of intense degradation. Contraction mainly took place on the tongue and right side of the glacier because they are open to the Sun and there are no rock cliffs that would provide avalanches. The main contraction of the glacier area occurred in 1989-2000 and up to 2008, the maximum reduction of the glacier length was observed in 1989-2000 (Fig. 40).
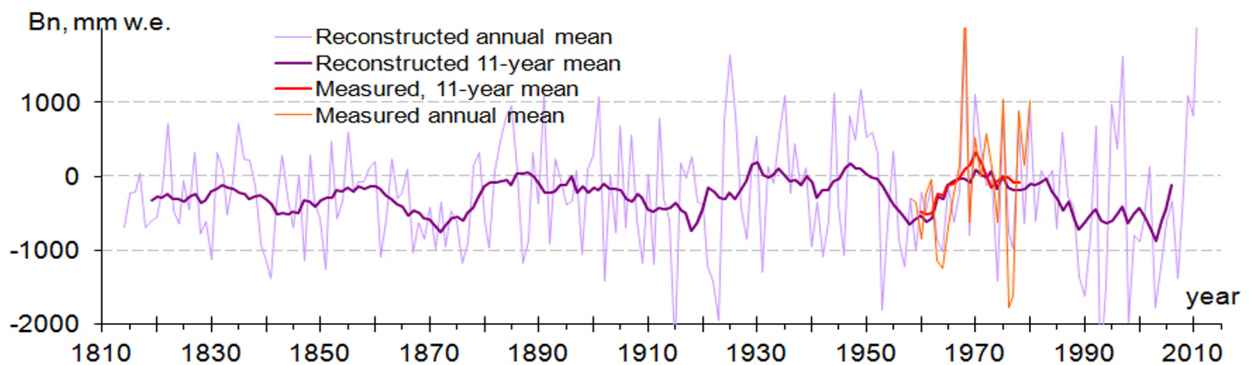


Figure 38. Mass balance of the IGAN glacier for the last 200 yr, annual and average for 11 yr [Ivanov 2009, added].

By processing the surface layer data and the results of the DGPS survey of the IGAN glacier performed by Nosenko and Murav'ev, a map of the glacier surface height in the period between 1963 and 2008 was composed (Fig. 41). Based on this map, the changes in the IGAN glacier volume for 45 years were estimated. This map is a continuation of similar maps (Figs. 42, 43) composed previously by Tsvetkov [Atlas of Snow and Ice Resources 1997; Atlas of the YNAD 2004].

The Khar-Naurdy-Keu plateau, which has an area of about 1 km², is completely covered by large detrital rocks. In the eastern part, it is complicated by a series of moderate-size highland terraces (1-2 m high) going down step by step to the slope part of the IGAN glacier (Fig. 44). Snowfields stay on the terrace steps (at some places, almost until the end of summer), which favor the development of frost-solifluction denudation, which leads to flattening of the mountain top and entrainment of the fragmentation products toward the glacier. These processes are particularly well expressed on the ridge of the northern wall of the kar, which separates the latter from the steep slope to the B. Khadata lake. The eastern part of the ridge is an inclined area up to 250 m wide with numerous terraces. In the western direction, the area becomes

FIGURE. 39. Topography of the IGAN glacier, measurements in 1953 and 1982. Glacier boundary: 1 – 1953; 2 – 1981; isolines: 3 – 1953; 4 – 1981; 5 – kinematic boundary of alimentation zone; 6 – isolines of the ice surface height (m); 7 – moraine; 8 – lake (1953); 9 – stream; 10 – lake (1983); 11 – contact boundary between slope and kar-valley parts; 12 – ice divide [Knizhnikov et al. 2007].
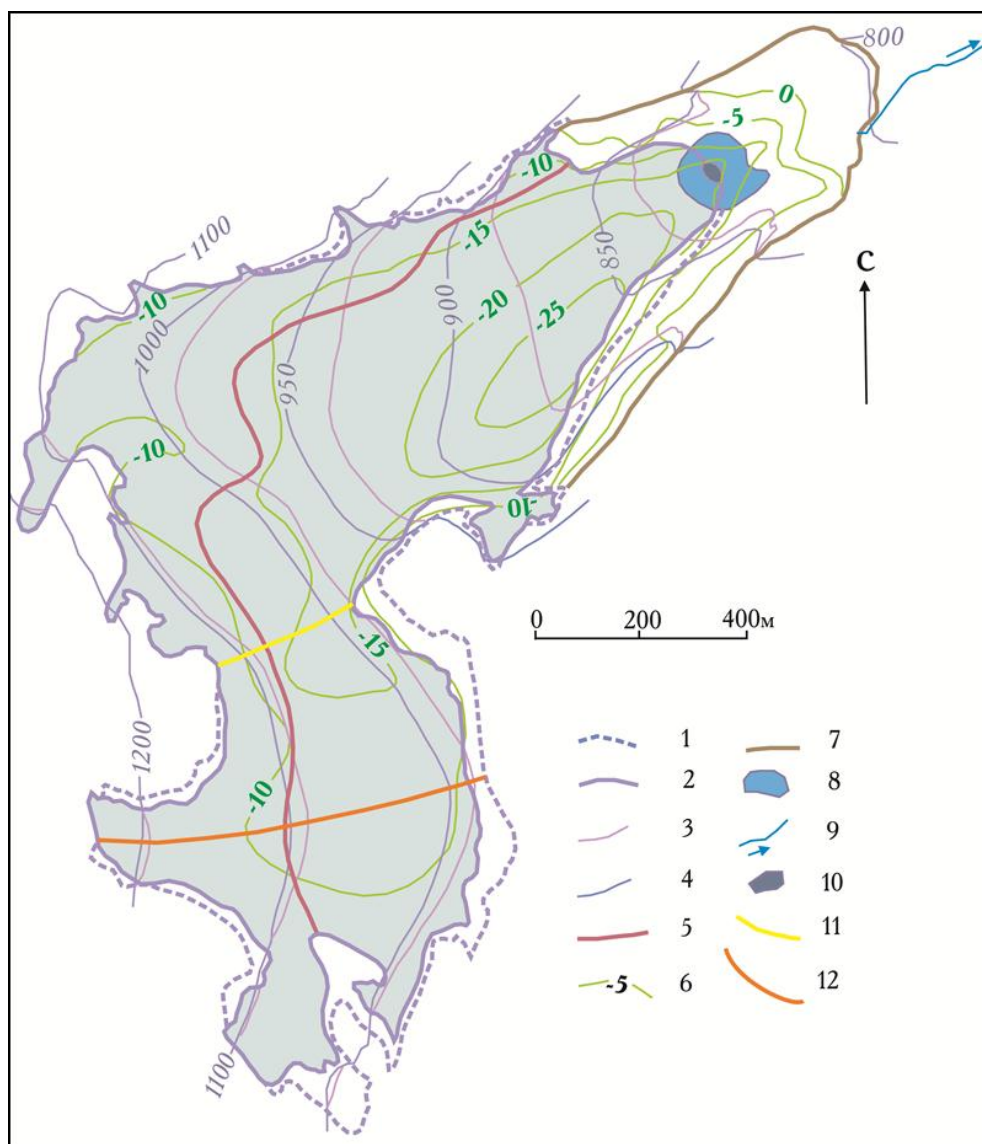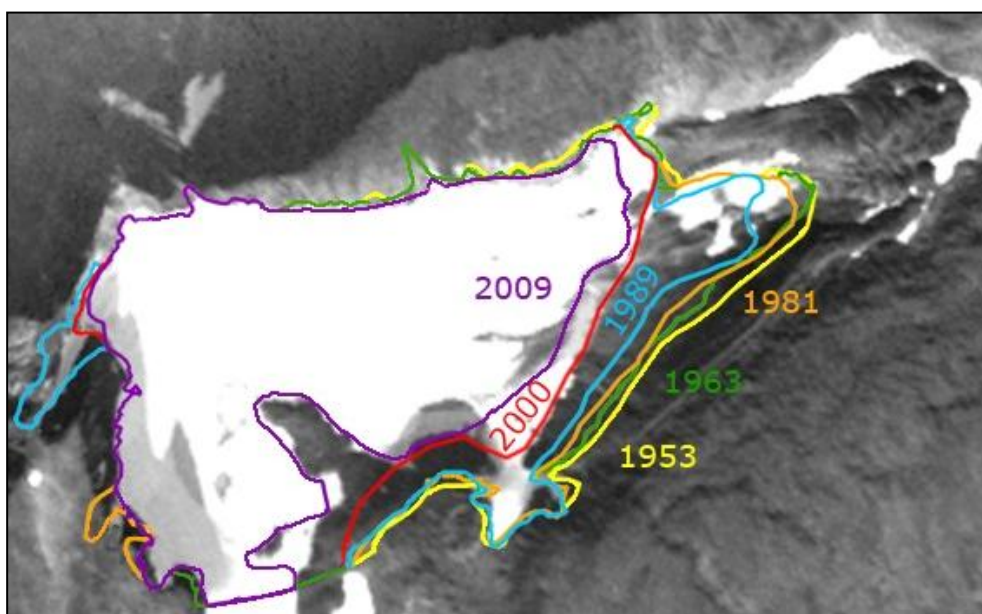


Figure 40. Boundary of the northern kar-valley glacier part in 1953, 1963, 1981, 1989, 2000, 2009 yr, spacephoto SPOT 5 2009.
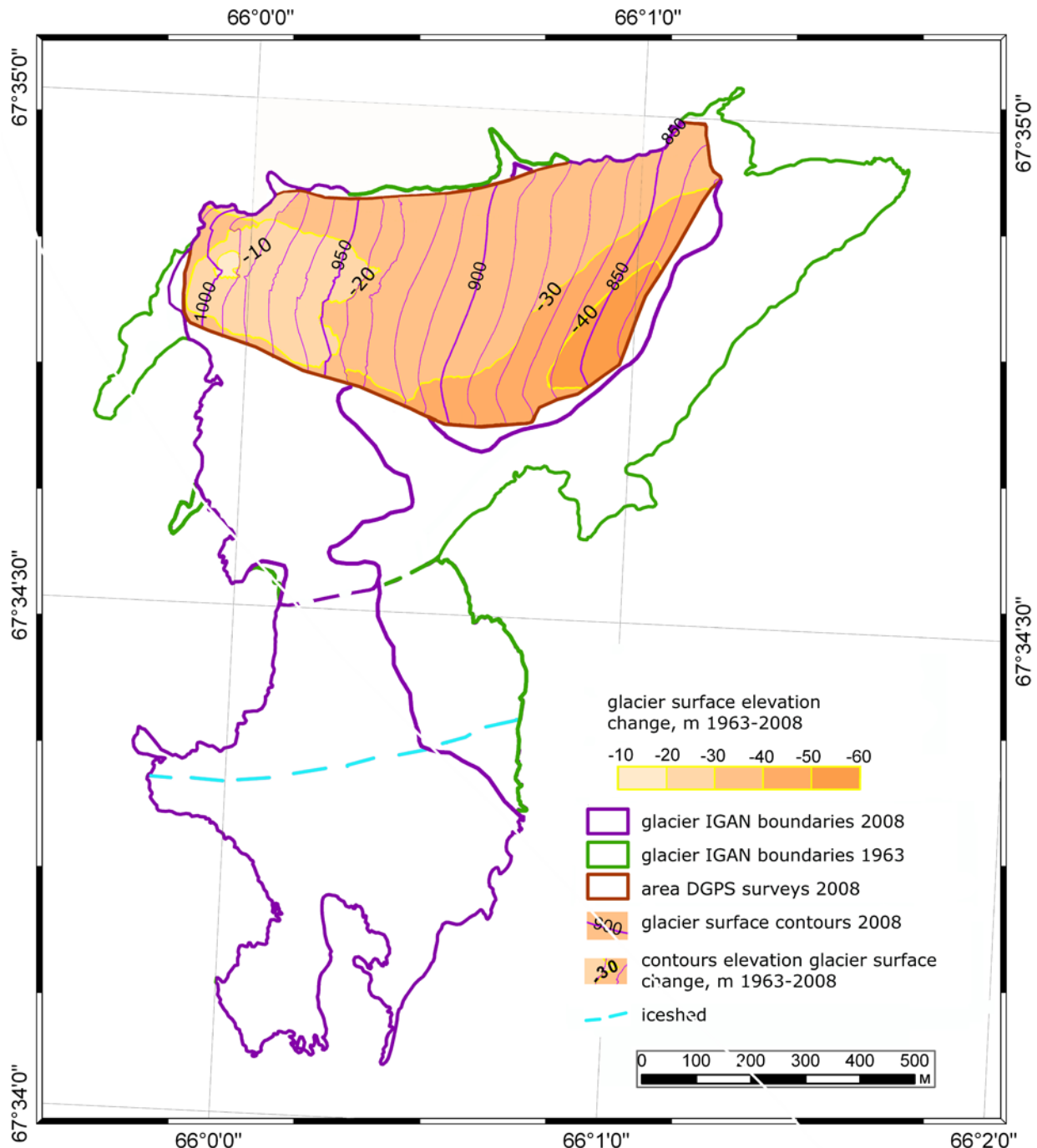
Figure 41. IGAN glacier degradation in 1963-2008.

narrower and transforms to a sharp ridge with three well-expressed peaks on the top. The development of a system of highland terraces on the inclined surface of this area leads to ridge truncation. It looks as if the highland terraces "undercut" the kar ridge and "attack" it. This, on the one hand, the kar erosion processes and erosive dissection create kar ridges, peaks, and make the relief sharper as a whole; on the other hand, the frost-solifluction denudation assists in flattening and rounding of sharp shapes. The action of these two oppositely directed processes finally make the summits lower.
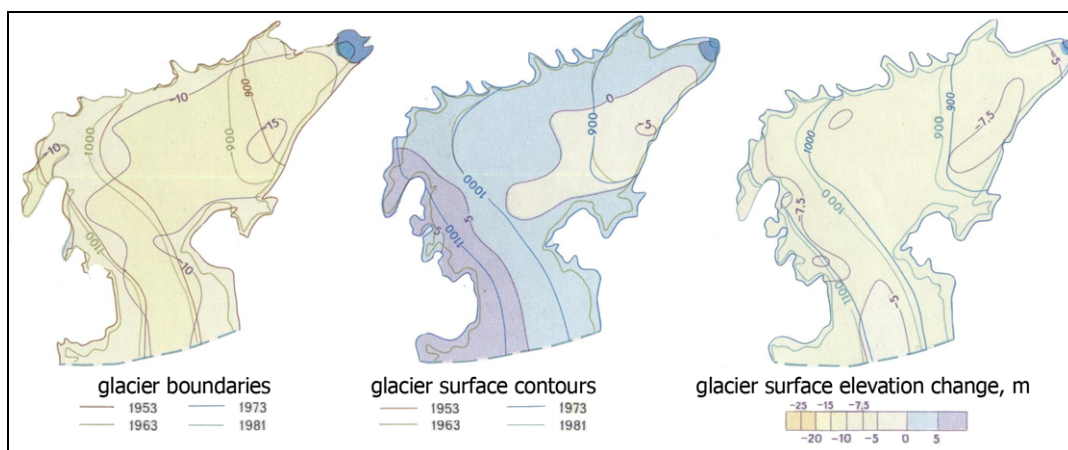
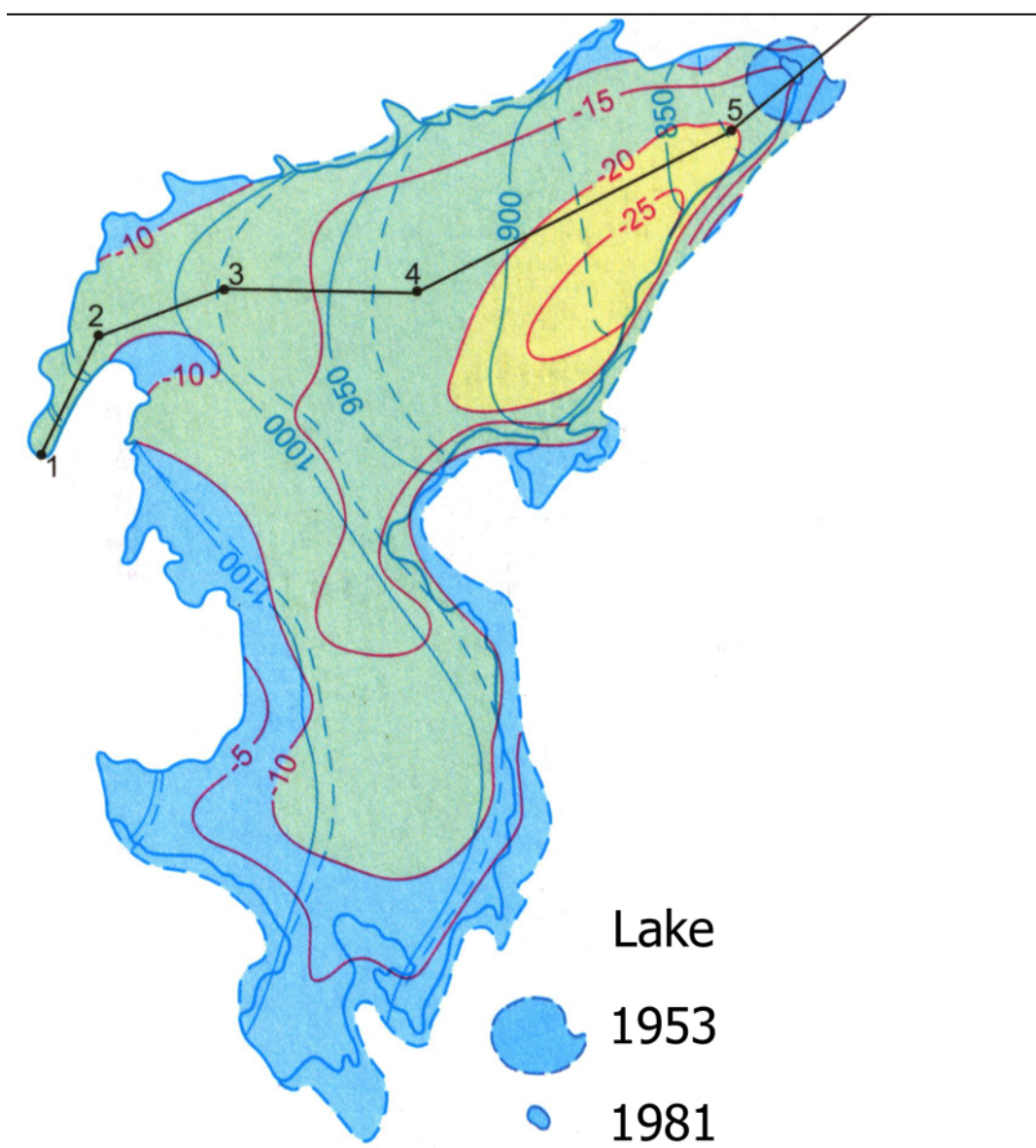FIGURE 42. Change of the surface height, IGAN glacier [Atlas…1997].



FIGURE 43. Change of the surface height, IGAN glacier (1953-1981) гг.
[Atlas of the YNAD 2004].

The IGAN plateau with an area of about 6 km² is more flat and is mainly covered by clay-detrital and stony residual rocks with a polygonal and spotted structure of the surface. Macrofragmental deposits are encountered sometimes. Clay-detrital eluvium on areas with considerable humidity, especially near the slopes, has the character of drifting sand after thawing. The presence of even very gentle slopes (3-5°) leads to the formation of solifluction jet flows. Their surface is a system of alternating shallow depressions and elevations (up to 0.2-0.3 m) parallel to the surface slope. Intense development of alluvial solifluction terraces is observed at steeper slopes, for instance, on the descent to the Gena-Khadata river; the height of the steps reaches 2 m. Typical stone runs are well developed on steep slopes descending toward the B. Khadata lake.
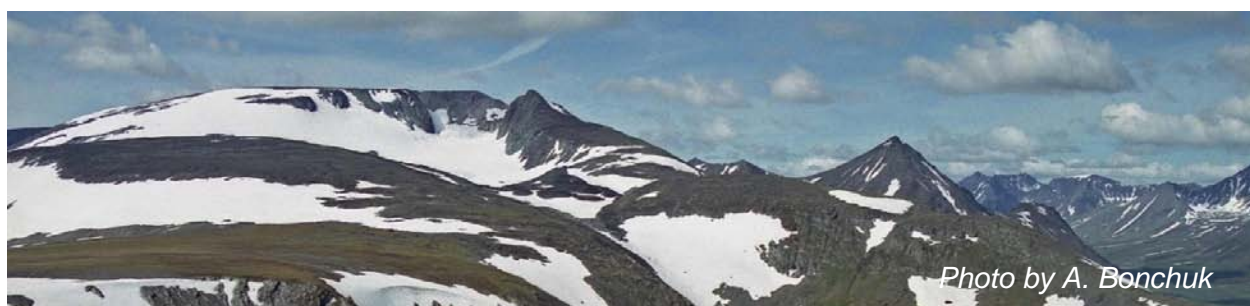


*Photo by A. Bonchuk*

FIGURE 44. View at m. Khar-Naurdu-Keu, IGAN glacier, IGAN plateau, 2005.

## CHAPTER 6. GLACIATION HISTORY.

Terminal moraines were studied in detail in the mountains and adjacent valleys. Investigations performed during the activities of the Polar-Ural Expedition showed that Polar Ural glaciation in late Pleistocene had a mountain-valley type [Ural Glaciation 1966]. Based on glaciogeomorphological research, spore and pollen analysis (Fig. 46), and radiocarbon dating, it was found that glaciers contracted stage by stage after late Dryas, disappeared in the Holocene optimum period [Surova et al. 1975], appeared again in the Neoglacial period, and reached the greatest area in the Little Ice Age.

Stadial moraines in the Urals were investigated by Maksimov [Maksimov 1970] who identified 6-8 stages in the valleys of the M. Paypudyna, Sob', and other rivers and constructed the time curve of Polar Ural deglaciation. Based on an incomplete set of stadial moraines, however, the same author concluded that there was an uplift of the Urals in Holocene by 800 m, which does not seem possible. In 1971-1973, ancient glaciation of the Polar Ural was studied by a team headed by Troitskii [Troitskii 1976].

The main attention was paid to propagation of stadial moraines (Figs. 45-47), sediments of supported englacial lakes and their interaction with terminal moraines, effect of glaciation on reconstruction of the hydrographical network in the mountains, and other issues.

Observations of glaciologists of the Institute of Geography are supported by the activities of the Russian-Norwegian project ICEHUSE (Ice Age development and Human Settlement in northern Eurasia) within the International Polar Year in 2007-2009. The project activities included drilling in several lakes, and the cores are now under analysis [Svendson 2011]. The datings of terminal moraines of the Chernov glacier [Mangerud 2008] and MGU glacier named after the Moscow State University [Svendson 2011], which were obtained on the basis of cosmogenic isotopes of beryllium-10 for the first time in the Urals, show that the size of the Polar Ural glaciers increased insignificantly in the last maximum of late Pleistocene glaciation (18-20 thousand years ago); they were only 1 km longer than now. Owing to the detailed description, we managed to find the place of sample collection at the foreground of the Chernov glacier in 2000 [Mangerud et al. 2008] and established that sample No. 2425 was indicated with incorrect coordinates; in reality, it is much closer to the glacier, at the point with the coordinates N67°37.396, E65°47.123. If this error is corrected, the samples arrange the terminal moraine banks into a sequence from 14.2 to 27.9 thousand years, except for the sample dated at 21.7 thousand years, which was possibly incorrectly taken from the slope fragment.

Concerning the history of glaciation in late Pleistocene, scientists still discuss whether the Polar Ural was the center of inland ice in cryochrons or only mountain-valley glaciation developed here. The discussion is not finished for various reasons: findings of the remnants of ancient human camps, marine deposits, disputable genesis of ice deposits on submountain valleys, terminal moraine banks, insufficient amounts of reliable datings of the absolute age, etc. In one of the recent publications dealing with this issue [Mangerud et al. 2008], there is a diagram with dating of large boulders in the valleys on the basis of beryllium-10 isotopes, which testifies to the mountain-valley character of glaciation in these periods.

The above-described circumstances require new comprehensive studies with involvement of specialists investigating various aspects of the Quarterly period.
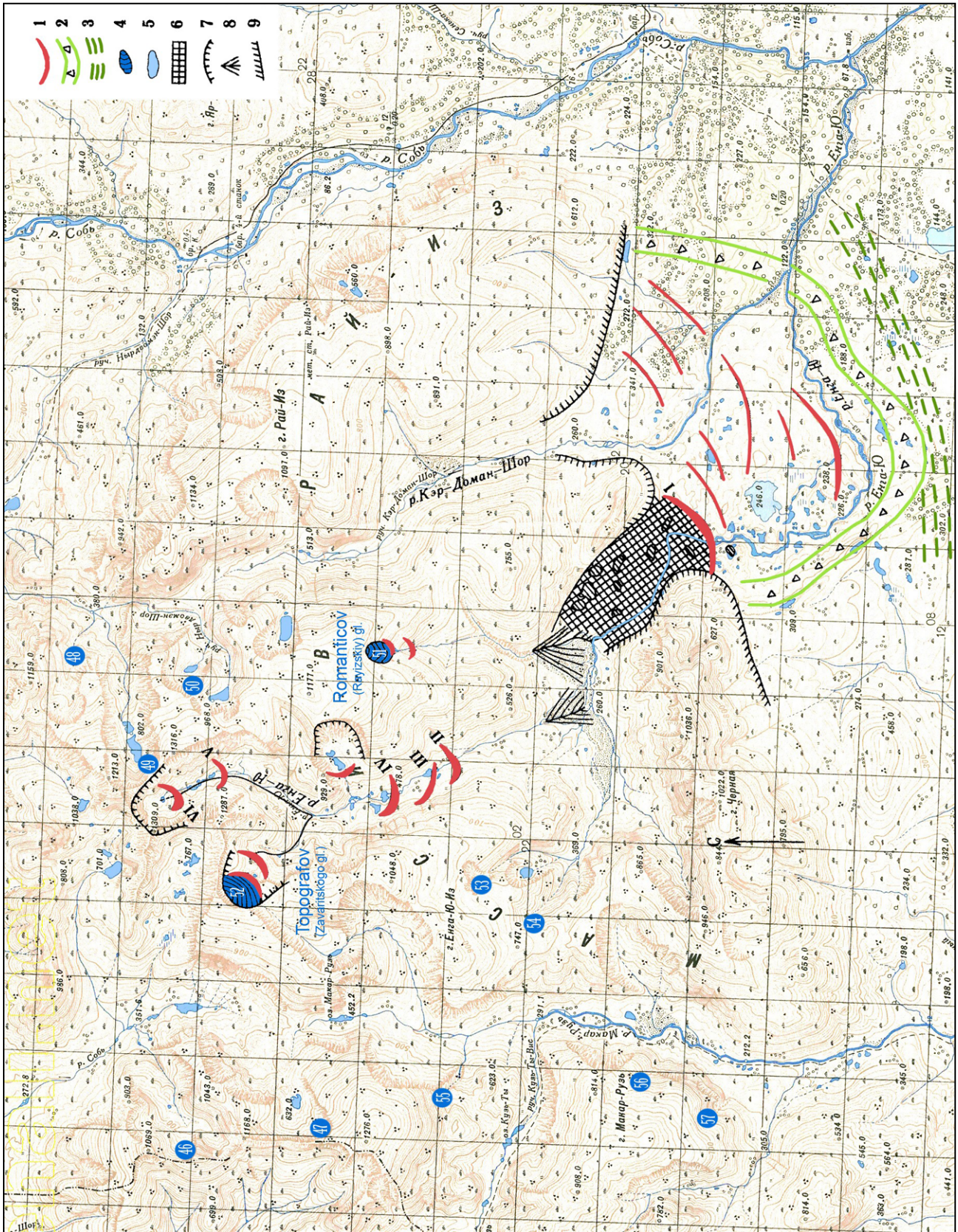
FIGURE 45. Moraine relief, Yenga-Yu river (Ray-Iz):
1 – stadial moraine; 2 – internal moraine banks; 3 – external moraine banks; 4 – existing glaciers; 5 – lakes; 6 – ice-dammed lake deposits; 7 – kars, 8 – debris fans; 9 – foothills [Troitskii 1976, added].

Контур ультрамафитового массива Рай-Из

Зоны тектонического меланжа Уральского коллизионного шва:
1- в подошве массива Рай-Из
2- в подошве Хараматалоуского метаморфического блока

Контуры моренных полей:
А - в долине реки Енга-Ю
В - в долине реки Собь

Ледники: 1- Романтиков
2-Топографов

Месторождение хромовых руд "Центральное"

Рудная точка А.Н.Заварицкого (1925г.) - первая находка хромитов на Рай-Изе

Контур ландшафтно-геологического памятника природы "Нырдвомен-Шор"

Места разбивки лагерей: 1-базовый
2- маршрутный (однодневный)

Линии экскурсионных маршрутов

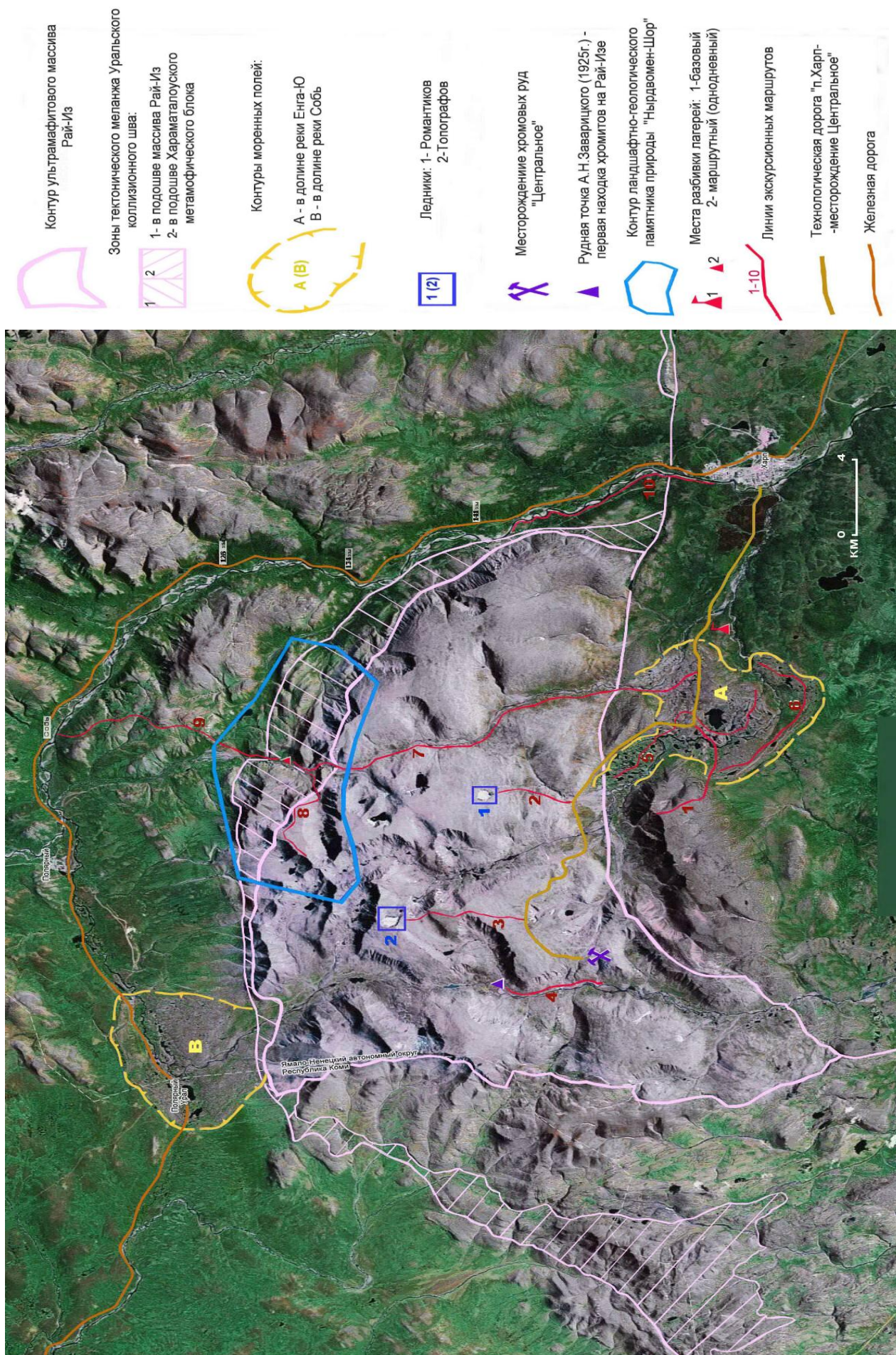Технологическая дорога "п.Харп--месторождение Центральное"

Железная дорога

FIGURE 46. Ray-Iz

FIGURE 47. Yeng-Yu river valley.



FIGURE 48. Romantikov glacier, 2011.

## References

Alisov B.P. Climate of the USSR, Moscow State University, Moscow, 1956, 128 pp.

Atlas of Snow and Ice Resources in the World, Russian Academy of Sciences, Moscow, 1997, 392 pp.

Atlas of the Yamal-Nenets Autonomous District. Polar Ural Glaciation, Tsvetkov D.G., Osipova G.B., Omskaya Kartograf. Fabrika, Omsk, 2004, pp.170–171.

Voloshina A.P. Some results of studying the mass balance of Polar Ural glaciers, VINITI, Moscow, 1988, pp. 48-51.

Ivanov M.N. Evolution of Polar Ural glaciations for the last 200 years, in: Glaciology at the Beginning of the 21st Century, Proc. Intern. Conf., Universitetskaya Kniga, Moscow, 2009, pp. 186-192.

Catalog of Glaciers of the USSR, Vol. 3. Northern Region, Part 3, Ural (L.S. Troitskii), Gidrometeoizdat, Leningrad, 1966, pp. 1-42.

Koshkarova V.L., Karpenko V.L., Orlova V.A. Dynamics of vegetation and upper boundary of forest in Holocene in the Polar Ural, Ekologiya, 1999, No. 2, pp.121–125.

Maksimov E.V. Stages of ancient glaciations and recent tectonics in the Putoran mountains, in the Polar and Nether-Polar Ural, Reports of the Geographical Society of the USSR, Leningrad, No. 16, 1970.

Materials of Observations in Mountain-Glacier Basins in the International Geographical Decade in the USSR, Part 1 (1965-1969), Gidrometeoizdat, Leningrad, 1980, 236 pp., Part 2 (1969-1974), Gidrometeoizdat, Leningrad, 1987, 300 pp.

Ural Glaciation (Troitskii L.S., Khodakov V.G., Mikhalev V.I., Gus'kov A.S., Lebedeva I.M., Adamenko V.N., Zhivkovich L.A., Nauka, Moscow, 1966, 307 pp.

Popov A.I. Permafrost Phenomena in the Earth Crust, Moscow State University, Moscow, 1967, 304 pp.

Surova T.G., Troitskii L.S., Punning Ya.M. Paleography and absolute chronology of the Holocene of the Polar Ural, Reports of the Academy of Sciences of the Estonian Republic, Chemistry, Geology, Vol. 24, No. 2, Tallin, 1975, pp. 152-159.

Troitskii L.S. Materials of Glaciological Research. International Geographical Year. Polar Ural. Glaciogeomorphology, VINITI, Moscow, 1962, 166 pp.

Troitskii L.S. Glacial Morphogenesis and History of Polar Ural Glaciation in Late Pleistocene and Holocene, Materials of Glaciological Research, No. 28, VINITI, Moscow, 1976, pp. 39-54.

Khodakov V.G. Water-Ice Balance in Regions of Modern and Ancient Glaciations of the USSR, Nauka, Moscow, 1978, 196 pp.

Tsvetkov D.G. Ten Years of Photogeodesic Activities on Polar Ural Glaciers, Materials of Glaciological Research, No. 16, Academy of Sciences of the USSR, Moscow, 1970, pp. 245-257

Tsykin E.N. Reconnaissance study of temperatures of the IGAN glacier in the Polar Ural, Glaciological Research No. 5, Academy of Sciences of the USSR, Moscow, 1960, pp. 109-116.

Shiyatov S.G. Dynamics of Woody and Shrub Vegetation in the Polar Ural Mountains under the Influence of Modern Changes in Climate, Urals Branch, Russian Academy of Sciences, Ekaterinburg, 2009, 216 pp.1.